Characteristics/finite element analysis for two incompressible fluid flows with surface tension using level set method

Sarra Maarouf, C. Bernardi, Driss Yakoubi

Version of Record: https://www.sciencedirect.com/science/article/pii/S0045782522001530
Manuscript_3148c9561d531530ac63979bfc59bf36

Characteristics/finite element analysis for two incompressible fluid flows with surface tension using level set method.

S. Maarouf[b,d], C. Bernardi[a], D. Yakoubi[c,*]

[a] *Laboratoire Jacques–Louis Lions, Sorbonne Université & CNRS, France*
[b] *Université de Jijel, Laboratoire Analyse, optimisation et traitement de l'information, Ouled Aissa, 18000, Jijel, Algeria.*
[c] *Léonard de Vinci Pôle Universitaire, Research Center, 92 916 Paris La Défense, France*
[d] *Groupe Interdisciplinaire de Recherche en Éléments Finis de l'Université Laval, Département de Mathématiques et Statistiques, Université Laval, Québec, Canada*

Abstract

In this paper, we present and analyze a finite element level set method based on the method of characteristics for two phase flow. Surface tension effects are taken into account by the CSF approach. We first write the variational formulation of the problem and investigate its well-posedness. Next, for the discretization, a first order method of characteristics approach for the evolution of the level set function and for the material derivative of the velocity is used. The velocity and pressure unknowns are discretized by $P2-P1$ Taylor–Hood finite elements. Then, in each time step, the interface transport is decoupled from the Navier–Stokes equations. Well–posedness results for subproblems in this decoupled discrete problem are derived. Furthermore, under high regularity assumptions, we state error estimates for our scheme. Ultimately, three computational examples illustrate the performance of the proposed method.

Keywords: Two phase flow, Level set method, finite element discretization, characteristics method.
2000 MSC: 76D05, 65M60, 35Q35

1. Introduction

Problems with free surfaces appear in immiscible multi-fluids, motion of glaciers, fluid structure interactions, blood in moving arteries and many other domains. Numerical methods for solving such problems are of great importance in many engineering applications and are still a challenging field. In recent years, analytical and numerical researches have been extensively studied and attained remarkable results, see for instance [14, 37] and references therein.

A challenging problem in numerical simulation of two immiscible fluids is then the motion of the free interface. There are two classifications of numerical methods in solving binary fluids: sharp interface and diffuse interface approaches. In the sharp approach, the fluid thermophysical properties such as density and viscosity experience a sharp transition at the interface between two fluids, whereas a smooth transition of fluid thermophysical properties happens in the case of diffuse interface approach. We refer the interested reader of the diffuse interface and their finite element analysis to [3, 4, 15, 19–21, 26].

In this work, the time-dependent Navier-Stokes equations govern the fluid motion in both fluids. Each fluid has a constant density and viscosity. As we are dealing with flow with more than one fluid, the surface tension at the fluid interface has to be taken account. We make use of sharp interface approach to track this interface. The surface tension is modelled as a body force concentrated at the interface by employing the Continuum Surface Force (CSF) model of Brackbill et al. [9]. The CSF model allows us to treat the dynamic

*Corresponding author
Email addresses: sarra.maarouf@univ-jijel.dz (S. Maarouf), driss.yakoubi@devinci.fr (D. Yakoubi)

boundary condition at the interface implicitly. For example, if φ describes the position of the interface, the basic equation underlying this method is:

$$\frac{\partial \varphi}{\partial t} + \boldsymbol{u} \cdot \nabla \varphi = 0. \tag{1.1}$$

Function φ can be taken (for instance) positive in one fluid and negative in the other whereas $\boldsymbol{u}$ is a given velocity field assumed divergence-free.

Since the nature of equation (1.1) is hyperbolic, some oscillations may appear near discontinuities of φ and numerical scheme may bring spurious diffusion, which implies an imprecise determination of the position of the interface. There are many numerical schemes which have been developed to address this difficulty. For example, moving interfaces can be handled with the Level Set method introduced S. Osher and al. [31, 40], see also [30] for a more general review of all these results. The function φ is meant to be the signed distance function to the interface, which is implicitly defined as the zero set of φ.

It should be noted that the level set method is one of the several interface-tracking techniques used routinely for two immiscible incompressible flow simulations. Others are the front-tracking method, see for instance [34, 44], the boundary integral method [24] and the volume-of-fluid (VOF) method [9, 27, 28]. The main advantages of the level set method compared with other techniques are
(i) function φ is smooth (it has no discontinuities), which helps the numerical resolution of (1.1) with high accuracy;
(ii) the attractive simplicity of its mathematical formulation and computing, and
(iii) the ability of the method to simulate complex interfacial flows with strong surface tension effects.
Moreover, it seems that the signed distance function to the interface gives more information on the interface than the step function used in VOF approaches. Again, the difficulty lies in the fact that the solution to (1.1) does not remain the signed distance function to interface $|\nabla \varphi| \neq 1$. Then the solution becomes very steep or flat in some regions, which makes difficult the precise determination of the position of the interface. To solve this difficulty, a first idea is to modify the velocity field $\boldsymbol{u}$ in (1.1) away from interface, so that the solution remains closer to the signed distance function. Another idea in the spirit of the reconstruction step of the VOF method is to use a reinitialization step, in order to recover the signed distance function. This can be performed for example using the following fictitious dynamics:

$$\frac{\partial \varphi}{\partial t} = sgn(\varphi)\ (1 - |\nabla \varphi|)\,, \tag{1.2}$$

whose solution in the long time limit is the signed distance function to the zero set of the initial condition $\varphi(t = 0)$. Recently, Reusken [35] introduces a new redistancing method for level set functions. This method is based on a gradient recovery technique that results in approximations of $\nabla \varphi_h$, where φ_h is an approximation of φ. These approximations satisfy the condition of a quasi-normal field on Γ_h, which is the zero level set of φ_h. The redistancing method does not need a reconstruction of the zero level set φ_h. However, one difficulty of the level set method is to ensure the conservation of the mass of each fluid component, since (1.1) is not a conservation law. Two solutions are presented in [11]. The authors proposed two finite element implementations that do not present this ill behaviour. The first relies on a discontinuous Galerkin discretization, and the second is a stabilized continuous FEM implementation based on a stabilization method.

In the level set method, the surface tension force is traditionally modelled as a distributed body force, though concentrated in a band around the interface and arranged in such a way that the force has a maximum on the interface and decays rapidly with distance from it (see [39, 40]). Furthermore the width ε of this band can be taken proportional to the mesh size h as $\varepsilon \approx 1.5\, h$ (see [13, 22]). Thus, the variation of the surface tension across the interface may be described in terms of a regularized (smoothed) delta function with compact support. This approach removes the interface singularity from the standard continuum fluid flow equations and ultimately allows the surface tension to be modelled using standard numerical techniques on Eulerian grids. The jump in phase properties across the interface, such as density and viscosity, is correspondingly modelled using a regularized Heaviside function. So the full model consists in the time-dependent Navier–Stokes equations and a transport equation for the interface. A detailed description of a similar model can be found for instance in [22], see also the references therein.

In this work, we investigate the main properties of the model and in particular the existence of a solution in the non-realistic case where the velocity satisfies homogeneous boundary conditions. Next, we propose a discretization of it by the characteristics method in time (indeed each equation contains a convection term) and standard conforming finite elements in space. We perform the a priori analysis of the discrete problem and prove nearly optimal estimates of the error. We finally present some numerical experiments that confirm the interest of both the model and its discretization.
The outline of the paper is as follows:
– In Section 2, we explain and write the model.
– In Section 3, we write its variational formulation and investigate its well-posedness.
– Section 4 is devoted to the description of the discretization and the well-posedness of the discrete problem.
– Its a priori analysis is performed in Section 5.
– In Section 6, we present some numerical experiments.
The work herein is an expanded and revised version of Bernardi et al. [5].

2. Mathematical description

Let Ω be a bounded connected open set in $\mathbb{R}^d$, $d = 2$ or 3, with a Lipschitz-continuous boundary $\partial\Omega$. If we assume a domain Ω with two immiscible fluids F_i, $i = 1, 2$, then the time dependent subdomains $\Omega_i(t)$, $t \in (0, T_f), T_f > 0$ are bounded by an external boundary $\partial\Omega$ and by a dynamic interface $\Gamma(t)$, see Figure 1. We assume that both fluids are homogeneous and therefore the physical properties are constant in each Ω_i which are a bounded connected domain with a Lipschitz–continuous and connected boundary $\partial\Omega_i(t)$:

$$\overline{\Omega} = \overline{\Omega}_1(t) \cup \overline{\Omega}_2(t), \qquad \Omega_1(t) \cap \Omega_2(t) = \emptyset. \tag{2.3}$$

We also define the interface between the two fluids

$$\Gamma(t) = \partial\Omega_1(t) \cap \partial\Omega_2(t). \tag{2.4}$$

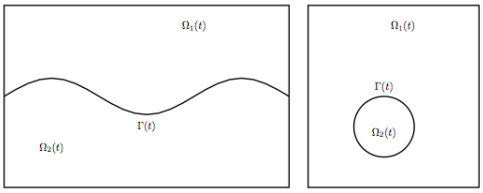

Figure 1: Two examples of domain Ω.

Then, the standard model for isothermal two immiscible flows can be described by the incompressible Navier-Stokes system in $\Omega \times (0, T_f)$

$$\begin{cases} \rho\left(\dfrac{\partial \boldsymbol{u}}{\partial t} + \boldsymbol{u} \cdot \nabla \boldsymbol{u}\right) + \nabla p - \nabla \cdot (\nu \nabla \boldsymbol{u}) = \boldsymbol{f} + \boldsymbol{f}_\sigma \\ \nabla \cdot \boldsymbol{u} = 0 \\ \dfrac{\partial \rho}{\partial t} + \nabla \cdot (\rho \boldsymbol{u}) = 0. \end{cases} \tag{2.5}$$

which contains an additional force term $\boldsymbol{f}_\sigma$ due to the surface tension σ at the free interface $\Gamma(t)$. The unknowns are the velocity $\boldsymbol{u}$ (more precisely, each $\boldsymbol{u}_i = \boldsymbol{u}|_{\Omega_i}$ is the velocity of the fluid F_i, $i = 1, 2$) and the pressure p, $\boldsymbol{f}$ denotes any body force such as gravitational acceleration. The density of each fluid is assumed to be constant at $t = 0$: *i.e* $\rho(\boldsymbol{x})|_{t=0} = \rho_i > 0$, where ρ_i is a given constant, for $i = 1, 2$.
Since $\dfrac{\partial \rho}{\partial t} + \nabla \cdot (\rho \boldsymbol{u}) = 0$, for all points $\boldsymbol{x} \in \Omega_i(t)$ and $\forall t > 0$, we have

$$\rho(\boldsymbol{x}, t) = \rho_i, \quad \text{for } i = 1, 2. \tag{2.6}$$

Concerning the viscosities, we assume that: $\nu|_{\Omega_i} = \nu_i$ where each ν_i is non-negative constant. Surface tension effects are taken into account through the following force balance at the interface $\Gamma(t)$

$$\boldsymbol{u}_1 = \boldsymbol{u}_2 \qquad \text{and} \qquad (\nu_1 \nabla \boldsymbol{u}_1 - p_1 I) \cdot \boldsymbol{n} + (\nu_2 \nabla \boldsymbol{u}_2 - p_2 I) \cdot \boldsymbol{n} = \sigma \kappa \boldsymbol{n}.$$

Here $\boldsymbol{n}$ is the unit normal at the interface pointing for instance into Ω_2, $\sigma \geq 0$ is the surface tension coefficient and $\kappa = \nabla \cdot \boldsymbol{n}$ is the curvature of the interface $\Gamma(t)$. The first condition implies continuity of the velocity across the interface, whereas the second describes the force balance on $\Gamma(t)$. To handle the curvature term, it is often to rewrite it as a volume force, that means $\boldsymbol{f}_\sigma = \sigma \kappa \boldsymbol{n} \delta_{\Gamma(t)}$, where $\delta_{\Gamma(t)}$ is the Dirac delta function localizing the surface tension forces to the interface $\Gamma(t)$. In Lafaurie et al. [27], the authors propose an other shape but still equivalent to this force by introducing the projection operator in the tangent plan: $I - \boldsymbol{n} \otimes \boldsymbol{n}$ and then writing

$$\boldsymbol{f}_\sigma = -\nabla \cdot T, \qquad \text{such that} \qquad T = \sigma (I - \boldsymbol{n} \otimes \boldsymbol{n}) \, \delta_{\Gamma(t)}.$$

According to the applied Continuous Surface Force (CSF) approach, see [9], we introduce the following smooth regularization of the Heaviside function for a small $\varepsilon > 0$,

$$H_\varepsilon(\psi) = \begin{cases} 0 & \text{if } \psi < -\varepsilon, \\ \frac{1}{2}\big(1 + \frac{\psi}{\varepsilon} + \frac{1}{\pi} \sin(\frac{\pi \psi}{\varepsilon})\big) & \text{if } -\varepsilon \leq \psi \leq \varepsilon, \\ 1 & \text{if } \psi > \varepsilon. \end{cases} \tag{2.7}$$

The smoothed density ρ and the viscosity ν are now given by

$$\rho(\varphi) = \rho_1 + (\rho_2 - \rho_1) H_\varepsilon(\varphi), \tag{2.8}$$
$$\nu(\varphi) = \nu_1 + (\nu_2 - \nu_1) H_\varepsilon(\varphi). \tag{2.9}$$

Since φ is a signed distance function (so that $\nabla \varphi$ is a normal vector to $\Gamma(t)$) and using the well-known expressions, this tensor T can also be written as a function of φ, as follows:

$$T(\varphi) = \sigma \frac{dH_\varepsilon(\varphi)}{d\varphi} (I - \nabla \varphi \otimes \nabla \varphi), \tag{2.10}$$

where $\nabla \varphi \otimes \nabla \varphi$ stands for the tensor with coefficients $\partial_{x_i} \varphi \, \partial_{x_j} \varphi$, $1 \leq i, j \leq d$.
We recall that the unit normal $\boldsymbol{n}$ to the interface is classically obtained via φ : On the curve $\Gamma(t)$ with equation $\varphi = 0$, $\boldsymbol{n} = \dfrac{\nabla \varphi}{|\nabla \varphi|}$.

Finally, the governing equations which describe two immiscible fluids with surface tension can be writing as a coupled time-dependent Navier–Stokes equations with transport equation in $\Omega \times (0, T_f)$

$$\begin{cases} \rho(\varphi) \left(\dfrac{\partial \boldsymbol{u}}{\partial t} + \boldsymbol{u} \cdot \nabla \boldsymbol{u} \right) + \nabla p - \nabla \cdot (\nu(\varphi) \nabla \boldsymbol{u})) + \nabla \cdot T(\varphi) = \boldsymbol{f} \\ \nabla \cdot \boldsymbol{u} = 0 \\ \dfrac{\partial \varphi}{\partial t} + \boldsymbol{u} \cdot \nabla \varphi = 0. \end{cases} \tag{2.11}$$

The last equation means that the interface $\Gamma(t)$ is convected by the fluid.

To make the problem complete, we enforce suitable boundary and initial conditions. The Dirichlet condition is imposed to the velocity and the level set function

$$\boldsymbol{u} = \boldsymbol{u}_D \quad \text{on } \partial\Omega \qquad \text{and} \qquad \varphi = \varphi_D \quad \text{on } \Gamma_{\boldsymbol{u}}, \tag{2.12}$$

where $\Gamma_{\boldsymbol{u}}$ denotes the part of boundary where the fluid goes in

$$\Gamma_{\boldsymbol{u}} = \{\boldsymbol{x} \in \partial\Omega; \, \boldsymbol{u}(\boldsymbol{x}, t) \cdot \boldsymbol{n}(\boldsymbol{x}) < 0\},$$

and the initial conditions obviously read

$$\boldsymbol{u}(\boldsymbol{x},0)=\boldsymbol{u}_0(\boldsymbol{x}) \quad \text{and} \quad \varphi(\boldsymbol{x},0)=\varphi_0(\boldsymbol{x}) \qquad \text{for a.e. } \boldsymbol{x}\in\Omega. \tag{2.13}$$

The existence of $\Gamma_{\boldsymbol{u}}$ and the boundary condition on φ come from the nature of the third line of (2.11) which is a hyperbolic equation. However, in the case of the non-slip condition on $\partial\Omega$ for $\boldsymbol{u}$, no essential boundary conditions are needed on the level set function. Certain compatibility conditions must be satisfied by the given data, mainly

$$\nabla\cdot\boldsymbol{u}_0=0 \quad \text{in } \Omega \qquad \text{and} \qquad \boldsymbol{u}_D(\cdot,0)\cdot\boldsymbol{n}=\boldsymbol{u}_0\cdot\boldsymbol{n} \quad \text{on } \partial\Omega, \tag{2.14}$$

in order to ensure the smoothness of the solution. From now on, we take φ negative on $\Omega_1(t)$ and positive on $\Omega_2(t)$, whence some compatibility conditions on φ_0 and φ_D.

3. Variational formulation and well-posedness

Of course, our dream would be that problem (2.11) provided with the initial and boundary conditions (2.12)- (2.13) is well-posed. However this seems impossible, for the two following reasons:
• very few existence results are known for the transport equation (third line in (2.11)) when the velocity $\boldsymbol{u}$ does not vanish on the boundary and they require too much regularity of the domain;
• the uniqueness of the solution of the time-dependent Navier-Stokes equation (first and second lines in (2.11)) is actually unknown in dimension $d=3$. So, we restrict ourselves to a simpler case.

In what follows, we use the whole scale of Sobolev spaces $W^{m,q}(\Omega)$, with $m\geq 0$ and $1\leq q\leq+\infty$, equipped with the norm $\|\cdot\|_{W^{m,q}(\Omega)}$ and seminorm $|\cdot|_{W^{m,q}(\Omega)}$, with the usual notation $H^m(\Omega)$ when $q=2$. We also need the space $H^1_0(\Omega)$ of functions in $H^1(\Omega)$ vanishing on $\partial\Omega$. For any separable Banach space E equipped with the norm $\|\cdot\|_E$, we denote by $\mathcal{C}^0(0,T_f;E)$ the space of continuous functions from $[0,T_f]$ with values in E. For each integer $m\geq 0$, we also introduce the space $H^m(0,T_f;E)$ as the space of measurable functions on $]0,T_f[$ with values in E such that the mappings: $v\mapsto\|\partial_t^\ell v\|_E$, $0\leq\ell\leq m$, are square-integrable on $]0,T_f[$. We refer to [1] for the main properties of all these spaces.

Let us first consider the transport equation. In the case where $\boldsymbol{u}_D$ is not zero, the only existence result can be found in [8, Thm VI.1.6] but it requires too much regularity of the domain Ω and of the velocity $\boldsymbol{u}$. So, even if the case $\boldsymbol{u}_D\cdot\boldsymbol{n}=0$ was treated in [12, Section IV.4], from now on we assume that

$$\boldsymbol{u}_D=\boldsymbol{0}. \tag{3.15}$$

With this condition, it is rather easy to prove the existence of a solution via the characteristics method, see [2, Thm II.7.6]. We are thus in a position to state the result concerning this equation.

Proposition 3.1. *Assume that the function $\boldsymbol{u}$ is divergence-free and satisfies*

$$\boldsymbol{u}\in\mathcal{C}^0(0,T_f;H^1_0(\Omega)^d)\cap\mathcal{C}^0(0,T_f;W^{1,\infty}(\Omega)^d). \tag{3.16}$$

Then, for any datum φ_0 in $L^2(\Omega)$, the problem

$$\begin{cases}\dfrac{\partial\varphi}{\partial t}+\boldsymbol{u}\cdot\nabla\varphi=0 & \text{in } \Omega\times(0,T_f),\\ \varphi(\cdot,0)=\varphi_0 & \text{in } \Omega,\end{cases} \tag{3.17}$$

admits a unique solution φ in $\mathcal{C}^0(0,T_f;L^2(\Omega))$. Moreover, this solution satisfies

$$\sup_{0\leq t\leq T_f}\|\varphi(\cdot,t)\|_{L^2(\Omega)}\leq\|\varphi_0\|_{L^2(\Omega)}. \tag{3.18}$$

Proof. We establish successively the existence, the uniqueness and the stability property (3.18) of the solution.

1) **Existence:** Owing to the property (3.16) of $\boldsymbol{u}$, applying the Cauchy–Lipschitz theorem [38, Th. 21.1] yields that there exists for every $(\boldsymbol{x},t)$ in $\Omega\times[0,T_f]$, a characteristic function $X=X(\boldsymbol{x},t;\cdot)$ in $\mathcal{C}^0(0,T;\mathbb{R}^d)$ solution of the ordinary differential equation

$$\begin{cases}\dfrac{dX}{dt}=\boldsymbol{u}\circ X & \text{in } \Omega\times(0,T_f),\\ X(\boldsymbol{x},t;t)=\boldsymbol{x} & \text{in } \Omega.\end{cases}$$

Thus, it is readily checked that the function φ defined by

$$\varphi(\boldsymbol{x},t)=\varphi_0(X(\boldsymbol{x},0;t)), \tag{3.19}$$

is a solution of problem (3.17).

2) **Uniqueness:** Let φ_1 and φ_2 be two solutions of problem (3.17). Setting $\varphi=\varphi_1-\varphi_2$ and multiplying the difference of the two equations by φ gives

$$\frac{1}{2}\frac{\partial\varphi^2}{\partial t}+\frac{1}{2}\boldsymbol{u}\cdot\nabla\varphi^2=0.$$

Since $\boldsymbol{u}$ is divergence-free and vanishes on the boundary, integrating on Ω yields

$$\frac{1}{2}\frac{d}{dt}\|\varphi\|^2_{L^2(\Omega)}=0,$$

whence, since $\varphi(\cdot,0)$ is zero, $\varphi(\cdot,t)$ is zero. Thus, φ_1 and φ_2 coincide.

3) **Stability:** Multiplying as previously (3.17) by φ and integrating on Ω leads to $\dfrac{d}{dt}\|\varphi\|^2_{L^2(\Omega)}=0$, whence property (3.18).

□

It follows from (3.19) that the regularity of φ depends only on that of $\boldsymbol{u}$ and φ_0. So we state the regularity properties that we need to study the full problem.

Corollary 3.2. *If the assumptions of Proposition* 3.1 *hold, for any real number q, $1\le q<\infty$, and for any datum φ_0 in $W^{1,q}(\Omega)$, the solution φ of problem* (3.17) *belongs to $\mathcal{C}^0(0,T_f;W^{1,q}(\Omega))$.*

We now consider the Navier-Stokes equations. Their variational formulation consist to find $(\boldsymbol{u},p)\in L^2(0,T;H^1_0(\Omega)^d)\cap\mathcal{C}^0(0,T;L^2(\Omega)^d)\times L^2(0,T;L^2(\Omega))$ such that

$$\boldsymbol{u}(\cdot,0)=\boldsymbol{u}_0, \tag{3.20}$$

and for a.e. $t\in[0,T]$ and for all $(\boldsymbol{v},q)\in H^1_0(\Omega)^d\times L^2(\Omega)$

$$\begin{aligned}&\int_\Omega\rho(\varphi)(\boldsymbol{x})\left(\frac{\partial\boldsymbol{u}}{\partial t}+\boldsymbol{u}\cdot\nabla\boldsymbol{u}\right)(\boldsymbol{x})\cdot\boldsymbol{v}(\boldsymbol{x})\,d\boldsymbol{x}-\int_\Omega(\nabla\cdot\boldsymbol{v})(\boldsymbol{x})p(\boldsymbol{x})\,d\boldsymbol{x}\\&\quad+\int_\Omega\nu(\varphi)(\boldsymbol{x})\nabla\boldsymbol{u}(\boldsymbol{x}):\nabla\boldsymbol{v}(\boldsymbol{x})\,d\boldsymbol{x}-\int_\Omega T(\varphi)(\boldsymbol{x}):\nabla\boldsymbol{v}(\boldsymbol{x})\,d\boldsymbol{x}=\langle\boldsymbol{f},\boldsymbol{v}\rangle,\\&\int_\Omega(\nabla\cdot\boldsymbol{u})(\boldsymbol{x})q(\boldsymbol{x})\,d\boldsymbol{x}=0,\end{aligned} \tag{3.21}$$

where $\langle\cdot,\cdot\rangle$ denotes the duality pairing between $H^1_0(\Omega)^d$ and its dual space $H^{-1}(\Omega)^d$. The arguments for proving its equivalence with the first two lines of (2.11) are fully standard, so we skip them.

To go further, we first note from the definitions (2.8) and (2.9) that, for any φ,

$$\min\{\rho_1,\rho_2\}\le\rho(\varphi)\le\max\{\rho_1,\rho_2\},\qquad\min\{\nu_1,\nu_2\}\le\nu(\varphi)\le\max\{\nu_1,\nu_2\}. \tag{3.22}$$

Next, since $\dfrac{dH_\varepsilon}{d\varphi}$ is bounded independently of φ, for any φ in $L^4(0,T_f;W^{1,4}(\Omega))$, the quantity $T(\varphi)$ belongs to $L^2(0,T_f;L^2(\Omega)^{d\times d})$. So all the terms in problem (3.21) are well-defined. Moreover, thanks to all these properties, the existence of a solution for problem (3.21) is derived by exactly the same arguments as for the standard Navier–Stokes equations. So we refer to [42, Chap. III, Thms 3.1 & 3.2] and [18, Chap. V, Thms 1.4 & 1.5] for the next result.

Proposition 3.3. *Assume that the function φ belongs to $L^4(0,T_f;W^{1,4}(\Omega))$. Then, for any datum $\boldsymbol{f}$ in $L^2(0,T_f;H^{-1}(\Omega)^d)$ and $\boldsymbol{u}_0$ in $L^2(\Omega)^d$ satisfying*

$$\nabla\cdot\boldsymbol{u}_0=0 \quad \text{in } \Omega \qquad \text{and} \qquad \boldsymbol{u}_0\cdot\boldsymbol{n}=0 \quad \text{on } \partial\Omega, \tag{3.23}$$

problem (3.20) – (3.21) has at least a solution $(\boldsymbol{u},p)$. Moreover, in dimension $d=2$, this solution is unique, up to an additive constant on the pressure.

Unfortunately, it seems difficult to prove, especially in dimension $d=3$, that this solution satisfies the regularity properties required in Proposition 3.1 (even if they could be weakened). Up to our knowledge, the only existence result for the full problem (3.17) – (3.20) – (3.21) is due to Milcent [29, Chap. IV, Th. 1]; we only quote it and refer to [29, Chap. IV] and [10, Thm 2.2] for its proof (which relies on space and time regularization).

Proposition 3.4. *Let Ω be a bounded smooth domain in $\mathbb{R}^3$, and let q be a real number >3. We consider data*
(i) φ_0 in $W^{2,q}(\Omega)$ such that $|\nabla\varphi_0|$ is larger than a positive constant in a neighbourhood of

$$\{\boldsymbol{x}\in\Omega;\ \varphi_0(\boldsymbol{x})=0\};$$

(ii) $\boldsymbol{u}_0$ in $W^{2,q}(\Omega)^d\cap W_0^{1,q}(\Omega)^d$ which is divergence-free in Ω.
Then, there exists a positive number T_* only depending on the initial data such that problem (3.17)-(3.20)-(3.21) has a solution in $\Omega\times[0,T_*]$. Moreover, this solution satisfies

$$\begin{aligned}\boldsymbol{u}&\in L^\infty(0,T_*;W_0^{1,q}(\Omega)^d)\cap L^q(0,T_*;W^{2,q}(\Omega)^d),\\ \varphi&\in L^\infty(0,T_*;W^{2,q}(\Omega)),\qquad \nabla p\in L^q(0,T_*;L^q(\Omega)^d).\end{aligned}$$

Even if neither the assumptions of this proposition nor the results are very realistic, it leaves the hope that the problem we work with is reasonable.

4. The discrete problem and its well-posedness

To describe the discrete problem, we first need some notation. Next, we write it and prove its well-posedness.

4.1. Some notation

Since we intend to work with non-uniform time steps, we introduce a partition of the interval $[0,T_f]$ into subintervals $[t_{n-1},t_n]$, $1\le n\le N$, with $0=t_0<t_1<\cdots<t_N=T_f$. We denote by τ_n the time step t_n-t_{n-1}, by τ the N-tuple $(\tau_1,\dots,\tau_N)$ and by $|\tau|$ the maximum of the τ_n, $1\le n\le N$.
We assume that Ω is a polygon ($d=2$) or a polyhedron ($d=3$). For $0\le n\le N$, let $(\mathcal{T}_h^n)_h$ be a regular family of triangulations of Ω (by triangles or tetrahedra), in the sense that, for each h:
• $\overline{\Omega}$ is the union of all elements of $\mathcal{T}_h^n$;
• The intersection of two different elements of $\mathcal{T}_h^n$, if not empty, is a vertex or a whole edge or a whole face of both of them;
• The ratio of the diameter h_K of any element K of $\mathcal{T}_h^n$ to the diameter of its inscribed circle or sphere is smaller than a constant independent of h and n.

As usual, h_n stands for the maximum of the diameters h_K, $K \in \mathcal{T}_h^n$. We also denote by $\mathcal{V}_h^n$ the set of all vertices of elements of $\mathcal{T}_h^n$.

In what follows, c, c', ... are generic constants which may vary from line to line but are always independent of the τ_n and h_n. Also, we have decided to work with the Taylor–Hood finite element introduced in [41]. So, denoting by $\mathcal{P}_k(K)$ the space of restrictions to K of polynomials with d variables and total degree $\leq k$, we consider the finite element spaces

$$\mathbb{Y}_h^n = \big\{ v_h \in H^1(\Omega);\ \forall K \in \mathcal{T}_h^n,\ v_h|_K \in \mathcal{P}_2(K) \big\}, \quad \mathbb{X}_h^n = (\mathbb{Y}_h^n)^d \cap H_0^1(\Omega)^d, \tag{4.24}$$

$$\text{and} \qquad \mathbb{M}_h^n = \big\{ q_h \in H^1(\Omega);\ \forall K \in \mathcal{T}_h^n,\ q_h|_K \in \mathcal{P}_1(K) \big\}. \tag{4.25}$$

Finally we denote by $\mathcal{I}_h^n$ the Lagrange interpolation operator at the nodes of $\mathcal{V}_h^n$ with values in $\mathbb{M}_h^n$.

4.2. Discretization of the transport equation

For reasons which appear later on, we still work with homogeneous boundary condition on the velocity, i.e. we assume that (3.15) holds. We have decided to use the characteristics method to discretize the transport equation, as introduced and firstly analysed in [32].

Assuming that the datum φ_0 is continuous on $\overline{\Omega}$, we simply define

$$\varphi_h^0 = \mathcal{I}_h^0 \varphi_0. \tag{4.26}$$

Next, at time t_n, assuming that $\boldsymbol{u}_h^{n-1}$ and φ_h^{n-1} are known, we define for all $\boldsymbol{x}$ in $\mathcal{V}_h^n$

$$\boldsymbol{x}_h^n = \boldsymbol{x} - \tau_n \, \boldsymbol{u}_h^{n-1}(\boldsymbol{x}), \tag{4.27}$$

thus, we define $\tilde{\varphi}_h^n$ by

$$\tilde{\varphi}_h^n(\boldsymbol{x}) = \varphi_h^{n-1}(\boldsymbol{x}_h^n), \tag{4.28}$$

and finally

$$\varphi_h^n = \mathcal{I}_h^n \tilde{\varphi}_h^n. \tag{4.29}$$

The simplicity of this algorithm is obvious. Note simply that:
(i) If $\boldsymbol{x}$ belongs to $\partial\Omega$, the fact that $\boldsymbol{u}_h^{n-1}$ belongs to $H_0^1(\Omega)^d$ implies that $\boldsymbol{x}_h^n$ is equal to $\boldsymbol{x}$, hence belongs to $\overline{\Omega}$;
(ii) otherwise, τ_n must be chosen small enough for $\boldsymbol{x}_h^n$ to be in $\overline{\Omega}$. This condition is made precise later on.

Remark 4.1. *Since the function φ_h^n is continuous on $\overline{\Omega}$, we can define the curve*

(4.30)

We hope that this curve is a good approximation of the interface $\Gamma(t)$ at time $t = t_n$. This will be investigated later on.

Remark 4.2. *It is well known that the interpolation (4.29) is very diffusive approach. Then, we can use the following L^2 projection:*

$$\int_\Omega \varphi_h^n(\boldsymbol{x})\, \psi(\boldsymbol{x})\, d\boldsymbol{x} = \int_\Omega \tilde{\varphi}_h^n(\boldsymbol{x})\, \psi(\boldsymbol{x})\, d\boldsymbol{x}, \quad \forall \psi \in \mathbb{M}_h^n. \tag{4.31}$$

The following mathematical analysis will be valid. However, all simulations in Section 6 are performed using the L^2 projection (4.31).

4.3. Discretization of the Navier–Stokes equations

This discretization relies on two arguments: using the characteristics method for handling the convection term and a Galerkin method for the rest of the equation. As previously, assuming that the datum $\boldsymbol{u}_0$ is continuous on $\overline{\Omega}$, we simply define

$$\boldsymbol{u}_h^0 = \mathcal{I}_h^0 \boldsymbol{u}_0. \tag{4.32}$$

Next, at time t_n, $1 \le n \le N$, assuming that $\boldsymbol{u}_h^{n-1}$ and φ_h^n are known, still relying on equation (4.27), we define $\tilde{\boldsymbol{u}}_h^{n-1}$ as the interpolate in $(\mathbb{M}_h^n)^d$ of the values $\boldsymbol{u}_h^{n-1}(\boldsymbol{x}_h^n)$ at all nodes of $\mathcal{V}_h^n$ which belong to Ω. Then, the discrete problem reads: for all $(\boldsymbol{v}, q) \in \mathbb{X}_h^n \times \mathbb{M}_h^n$

Find $\boldsymbol{u}_h^n$ in $\mathbb{X}_h^n$ and p_h^n in $\mathbb{M}_h^n$ such that

$$\begin{aligned}
&\int_\Omega \rho(\varphi_h^n)(\boldsymbol{x}) \left(\frac{\boldsymbol{u}_h^n - \tilde{\boldsymbol{u}}_h^{n-1}}{\tau_n} \right)(\boldsymbol{x}) \boldsymbol{v}(\boldsymbol{x})\, d\boldsymbol{x} - \int_\Omega (\nabla \cdot \boldsymbol{v})(\boldsymbol{x}) p_h^n(\boldsymbol{x})\, d\boldsymbol{x} \\
&\quad + \int_\Omega \nu(\varphi_h^n)(\boldsymbol{x}) \nabla \boldsymbol{u}_h^n(\boldsymbol{x}) : \nabla \boldsymbol{v}(\boldsymbol{x})\, d\boldsymbol{x} - \int_\Omega T(\varphi_h^n)(\boldsymbol{x}) : \nabla \boldsymbol{v}(\boldsymbol{x})\, d\boldsymbol{x} = \langle \boldsymbol{f}(t_n), \boldsymbol{v} \rangle, \\
&\quad \int_\Omega (\nabla \cdot \boldsymbol{u}_h^n)(\boldsymbol{x}) q(\boldsymbol{x})\, d\boldsymbol{x} = 0.
\end{aligned} \tag{4.33}$$

4.4. Well-posedness of the discrete problem

To prove the well-posedness of problem (4.27)-(4.28)-(4.29), we must check that the $\boldsymbol{x}_h^n$ defined in (4.27) belongs to $\overline{\Omega}$. This is proved in [36, Prop.1], see also [33, Rem.3] when the following condition holds

$$\tau_n < \frac{1}{\|\boldsymbol{u}_h^{n-1}\|_{W^{1,\infty}(\Omega)^d}}. \tag{4.34}$$

However, we have no a priori control on the quantity $\|\boldsymbol{u}_h^{n-1}\|_{W^{1,\infty}(\Omega)^d}$. So we prefer to use the following modified algorithm:

1. if the quantity defined in (4.27) belongs to $\overline{\Omega}$, take $\boldsymbol{x}_h^n$ equal to it;
2. otherwise, take $\boldsymbol{x}_h^n$ equal to
$$\boldsymbol{x}_h^n = \boldsymbol{x} - t\, \boldsymbol{u}_h^{n-1}(\boldsymbol{x}), \tag{4.35}$$
for the smallest t in $[0, \tau_n]$ such that $\boldsymbol{x} - t\, \boldsymbol{u}_h^{n-1}(\boldsymbol{x})$ belongs to $\partial\Omega$.

Note that the modification introduced above is only used for a small number of nodes $\boldsymbol{x}$ which are very near to $\partial\Omega$. We are thus in a position to state the next proposition.

Proposition 4.3. *For any φ_0 continuous on $\overline{\Omega}$, problem (4.27) (or (4.35))-(4.28) -(4.29) has a unique solution φ_h^n in $\mathbb{M}_h^n$.*

The well-posedness of problem (4.33) relies on standard arguments: Defining $\boldsymbol{x}_h^n$ by (4.27) or (4.35) as previously, we know $\tilde{\boldsymbol{u}}_h^{n-1}$. We also observe that the quantity $T(\varphi_h^n)$ belongs to $L^2(\Omega)^{d\times d}$. So the following result is readily checked.

Proposition 4.4. *For any datum $\boldsymbol{u}_0$ continuous on $\overline{\Omega}$, problem (4.33) has a unique solution $(\boldsymbol{u}_h^n, p_h^n)$ in $\mathbb{X}_h^n \times \mathbb{M}_h^n$, up to an additive constant on the pressure p_h^n.*

Proof. When φ_h^n (and $T(\varphi_h^n)$), $\tilde{\boldsymbol{u}}_h^{n-1}$ and $\boldsymbol{f}$ are known, this problem results in a square linear system. So it suffices to prove that the only solution of the problem

$$\begin{aligned}
\forall \boldsymbol{v} \in \mathbb{X}_h^n, \quad &\int_\Omega \rho(\varphi_h^n)(\boldsymbol{x}) \frac{\boldsymbol{u}_h^n(\boldsymbol{x})}{\tau_n} \boldsymbol{v}(\boldsymbol{x})\, d\boldsymbol{x} - \int_\Omega (\nabla \cdot \boldsymbol{v})(\boldsymbol{x}) p_h^n(\boldsymbol{x})\, d\boldsymbol{x} \\
&\qquad + \int_\Omega \nu(\varphi_h^n)(\boldsymbol{x}) \nabla \boldsymbol{u}_h^n(\boldsymbol{x}) : \nabla \boldsymbol{v}(\boldsymbol{x})\, d\boldsymbol{x} = 0, \\
\forall q \in \mathbb{M}_h^n, \quad &\int_\Omega (\nabla \cdot \boldsymbol{u}_h^n)(\boldsymbol{x}) q(\boldsymbol{x})\, d\boldsymbol{x} = 0,
\end{aligned}$$

is zero, up to an additive constant on the pressure p_h^n. By taking $\boldsymbol{v}$ equal to $\boldsymbol{u}_h^n$, combining the two previous equations and using (3.22), we easily derive that $\boldsymbol{u}_h^n$ is zero. Thus, the fact that p_h^n is a constant follows from the inf-sup condition, see for instance [18, Chap. II, Thm 4.2],

$$\forall q \in \mathbb{M}_h^n,\ \int_\Omega q(\boldsymbol{x})\,d\boldsymbol{x} = 0, \qquad \sup_{\boldsymbol{v}\in\mathbb{X}_h^n} \frac{\int_\Omega (\nabla\cdot\boldsymbol{v})(\boldsymbol{x}) q(\boldsymbol{x})\,d\boldsymbol{x}}{\|\boldsymbol{v}\|_{H^1(\Omega)^d}} \geq \beta\,\|q\|_{L^2(\Omega)}, \tag{4.36}$$

where the constant β is positive. □

Remark 4.5. *The main advantage of the discretization that we propose is that it uncouples the computation of the φ_h^n and of the $\boldsymbol{u}_h^n$. However, this can lead to a lack of convergence for too large time steps or in the case of time oscillations of the solution. To remedy this, we can use an iterative algorithm as follows: At each time t_n, knowing φ_h^{n-1} and $\boldsymbol{u}_h^{n-1}$*
1. define $\varphi_h^{n,0}$ as equal to φ_h^{n-1} and $\boldsymbol{u}_h^{n,0}$ as equal to $\boldsymbol{u}_h^{n-1}$;
2. setting $\boldsymbol{x}_h^{n,k} = \boldsymbol{x} - \tau_n\,\boldsymbol{u}_h^{n,k-1}(\boldsymbol{x})$ or the modified version (4.35), we define $\varphi_h^{n,k}$ as the interpolate in $\mathbb{M}_h^n$ of the values $\varphi^{n,k-1}(\boldsymbol{x}_h^{n,k})$ at all nodes of $\mathcal{V}_h^n$ and similarly $\tilde{\boldsymbol{u}}_h^{n,k-1}$ as the interpolate in $\mathbb{M}_h^n$ of the values $\boldsymbol{u}^{n,k-1}(\boldsymbol{x}_h^{n,k})$ at all nodes of $\mathcal{V}_h^n$ which belong to Ω. Next, for all $(\boldsymbol{v},q)\in\mathbb{X}_h^n\times\mathbb{M}_h^n$ we find $(\boldsymbol{u}_h^{n,k},p_h^{n,k})$ in $\mathbb{X}_h^n\times\mathbb{M}_h^n$ solution of the following problem

$$\begin{aligned}
&\int_\Omega \rho(\varphi_h^{n,k})(\boldsymbol{x})\left(\frac{\boldsymbol{u}_h^{n,k}-\tilde{\boldsymbol{u}}_h^{n-1,k}}{\tau_n}\right)(\boldsymbol{x})\boldsymbol{v}(\boldsymbol{x})\,d\boldsymbol{x} - \lambda_k\int_\Omega (\nabla\cdot\boldsymbol{v})(\boldsymbol{x}) p_h^{n,k}(\boldsymbol{x})\,d\boldsymbol{x}\\
&\quad + \lambda_k\int_\Omega \nu(\varphi_h^{n,k})(\boldsymbol{x})\nabla\boldsymbol{u}_h^{n,k}(\boldsymbol{x}) : \nabla\boldsymbol{v}(\boldsymbol{x})\,d\boldsymbol{x} - \lambda_k\int_\Omega T(\varphi_h^{n,k})(\boldsymbol{x}) : \nabla\boldsymbol{v}(\boldsymbol{x})\,d\boldsymbol{x}\\
&\quad = \lambda_k\langle \boldsymbol{f}(t_n),\boldsymbol{v}\rangle, \qquad \textit{and}\\
&\int_\Omega (\nabla\cdot\boldsymbol{u}_h^{n,k})(\boldsymbol{x}) q(\boldsymbol{x})\,d\boldsymbol{x} = 0.
\end{aligned}$$

Parameters λ_k are positive chosen in order to ensure the consistency of the algorithm.
3. For a fixed integer K, we set: $\varphi^n = \varphi^{n,K}$ and $\boldsymbol{u}^n = \boldsymbol{u}^{n,K}$, and go back to step 1.

Analysis of this algorithm is nearly the same as for the previous problem (4.27) – (4.28) – (4.29) – (4.33), so that we skip it.

5. A priori error analysis

In this section, we still work with $\boldsymbol{u}_D = \boldsymbol{0}$ and we admit that, for all $\boldsymbol{x}$ in $\mathcal{V}_h^n$, the $\boldsymbol{x}_h^n$ defined in (4.27) belongs to $\overline{\Omega}$. Indeed, it is not so difficult in practice to satisfy condition (4.34): when $\|\boldsymbol{u}_h^{n-1}\|_{W^{1,\infty}(\Omega)^d}$ is larger, it is possible to work with a smaller τ_n in order to enforce this condition.

We first state a stability property for the discrete transport equation.

Lemma 5.1. *For any datum φ_0 continuous on $\overline{\Omega}$, the next property holds*

$$\|\varphi_h^n\|_{L^\infty(\Omega)} \leq \|\varphi_0\|_{L^\infty(\Omega)}, \qquad \textit{for } 1\leq n\leq N. \tag{5.37}$$

Proof. Since each φ_h^n belongs to $\mathbb{M}_h^n$, hence is piecewise affine, we have

$$\|\varphi_h^n\|_{L^\infty(\Omega)} = \max_{\boldsymbol{x}\in\mathcal{V}_h^n} |\varphi_h^n(\boldsymbol{x})|. \tag{5.38}$$

Thus it follows from (4.28) and (4.29) that

$$\|\varphi_h^n\|_{L^\infty(\Omega)} \leq \|\varphi_h^{n-1}\|_{L^\infty(\Omega)}.$$

By noting that

$$\|\mathcal{I}_h^0\varphi_0\|_{L^\infty(\Omega)} \leq \|\varphi_0\|_{L^\infty(\Omega)},$$

the desired result is derived by induction on n. □

The error estimate is a little more tricky, even in the L^∞- norm. We refer to [33, Prop. 1] for a similar result in a different case.

Proposition 5.2. *Assume that the solution φ of problem (3.17) satisfies*

$$\varphi \in \mathcal{C}^0(0,T_f;W^{2,\infty}(\Omega)) \cap W^{1,\infty}(0,T_f;L^\infty(\Omega)). \tag{5.39}$$

Then the following estimate holds for $1 \le n \le N$

$$\|\varphi(\cdot,t_n) - \varphi_h^n\|_{L^\infty(\Omega)} \le C\left(h_n^2 + \tau_n(1+\|\boldsymbol{u}_h^{n-1}\|_{L^\infty(\Omega)^d})\right) + \|\varphi(\cdot,t_{n-1}) - \varphi_h^{n-1}\|_{L^\infty(\Omega)}, \tag{5.40}$$

where the constant C only depends on the regularity of φ.

Proof. Let us start using the following triangle inequality

$$\|\varphi(\cdot,t_n) - \varphi_h^n\|_{L^\infty(\Omega)} \le \|\varphi(\cdot,t_n) - \mathcal{I}_h^n\varphi(\cdot,t_n)\|_{L^\infty(\Omega)} + \|\mathcal{I}_h^n\varphi(\cdot,t_n) - \varphi_h^n\|_{L^\infty(\Omega)}.$$

Bounding the first term in the right-hand side relies on standard results [6, Chap. IX, Lemme 1.1]. To bound the second one, we use (5.38) and for each $\boldsymbol{x}$ in $\mathcal{V}_h^n$, we compute

$$\begin{aligned}\mathcal{I}_h^n\varphi(\boldsymbol{x},t_n) - \varphi_h^n(\boldsymbol{x}) &= \varphi(\boldsymbol{x},t_n) - \varphi_h^{n-1}(\boldsymbol{x}_h^n)\\ &= \varphi(\boldsymbol{x},t_n) - \varphi(\boldsymbol{x}_h^n,t_{n-1}) + \varphi(\boldsymbol{x}_h^n,t_{n-1}) - \varphi_h^{n-1}(\boldsymbol{x}_h^n).\end{aligned}$$

From the definition of $\boldsymbol{x}_h^n$ and the Lipschitz continuity of φ, we derive

$$|\mathcal{I}_h^n\varphi(\boldsymbol{x},t_n) - \varphi_h^n(\boldsymbol{x})| \le c\tau_n(1+\|\boldsymbol{u}_h^{n-1}\|_{L^\infty(\Omega)^d}) + \|\varphi(\cdot,t_{n-1}) - \varphi_h^{n-1}\|_{L^\infty(\Omega)},$$

where c stands for the Lipschitz constant of φ on $\Omega\times]0,T_f[$. Combining all this gives the desired estimate. □

In view of the quantity $T(\varphi)$, we also need an estimate for $\|\varphi(\cdot,t_n) - \varphi_h^n\|_{W^{1,4}(\Omega)}$.

Proposition 5.3. *Assume that, for a real number $q \ge 1$, the solution φ of problem (3.17) satisfies*

$$\varphi \in \mathcal{C}^0(0,T_f;W^{2,q}(\Omega)). \tag{5.41}$$

Then the following estimate holds for $1 \le n \le N$

$$\begin{aligned}\|\varphi(\cdot,t_n) - \varphi_h^n\|_{W^{1,q}(\Omega)} \le C\,h_n + C\hbar_n^{-1}\tau_n(1+\ &\|\boldsymbol{u}_h^{n-1}\|_{L^\infty(\Omega)^d})\\ &+ c\hbar_n^{-1}\,\|\varphi(\cdot,t_{n-1}) - \varphi_h^{n-1}\|_{L^\infty(\Omega)},\end{aligned} \tag{5.42}$$

where $\hbar_n$ stands for the minimum of the diameters h_K, $K \in \mathcal{T}_h^n$.

Proof. We start once more from the triangle inequality

$$\|\varphi(\cdot,t_n) - \varphi_h^n\|_{W^{1,q}(\Omega)} \le \|\varphi(\cdot,t_n) - \mathcal{I}_h^n\varphi(\cdot,t_n)\|_{W^{1,q}(\Omega)} + \|\mathcal{I}_h^n\varphi(\cdot,t_n) - \varphi_h^n\|_{W^{1,q}(\Omega)}.$$

and use [6, Chap. IX, Lemme 1.2] to evaluate the first term. On the other hand, denoting by $\psi_{\boldsymbol{x}}$ the Lagrange function associated with each node in $\mathcal{V}_h^n$, switching to the reference element to evaluate the norm of this function in $W^{1,q}(\Omega)$ and using the fact, due the regularity of the family of triangulations, the support of each $\psi_{\boldsymbol{x}}$ only intersects the support of a finite number of other ones, we derive

$$\|\mathcal{I}_h^n\varphi(\cdot,t_n) - \varphi_h^n\|_{W^{1,q}(\Omega)}^q \le c\sum_{\boldsymbol{x}\in\mathcal{V}_h^n} |\mathcal{I}_h^n\varphi(\boldsymbol{x},t_n) - \varphi_h^n(\boldsymbol{x})|^q\, h_{K_{\boldsymbol{x}}}^{d-q},$$

where $K_{\boldsymbol{x}}$ is any element of $\mathcal{T}_h^n$ containing $\boldsymbol{x}$. The maximum of the $|\mathcal{I}_h^n\varphi(\boldsymbol{x},t_n) - \varphi_h^n(\boldsymbol{x})|$ has been evaluated in the previous proof. We derive from the regularity of the family of triangulations that

$$\sum_{\boldsymbol{x}\in\mathcal{V}_h^n} h_{K_x}^d \le c\,\mathrm{meas}(\Omega),$$

which leads to the desired result. □

We are now interested in the evaluation of the error issued from the discrete Navier–Stokes equations. We refer to [7, Section 4.3] for this evaluation in a simpler case. We begin with the terms involving φ_h^n and, for simplicity, we denote by ε_1^n and ε_2^n the right-hand sides of estimates (5.40) and (5.42), respectively.

Lemma 5.4. *If the assumptions of Propositions* 5.2 *and* 5.3 *are satisfied, the following estimates hold for* $1 \le n \le N$

$$\|\rho(\varphi(.,t_n)) - \rho(\varphi_h^n)\|_{L^\infty(\Omega)} + \|\nu(\varphi(.,t_n)) - \nu(\varphi_h^n)\|_{L^\infty(\Omega)} \le \frac{\varepsilon_1^n}{\varepsilon}, \tag{5.43}$$

$$\textit{and} \qquad \|T(\varphi(.,t_n)) - T(\varphi_h^n)\|_{L^2(\Omega)^{d\times d}} \le c\,\big(\frac{\varepsilon_1^n}{\varepsilon^2} + \frac{\varepsilon_2^n}{\varepsilon}\big). \tag{5.44}$$

Proof. The two quantities in the left hand side of (5.43) can be estimate using the fact that H_ε is Lipschitz-continuous (the norm of its derivative is bounded by $\frac{1}{\varepsilon}$).
To prove (5.44), we use the triangle inequality

$$\begin{aligned}
&\|T(\varphi(.,t_n)) - T(\varphi_h^n)\|_{L^2(\Omega)^{d\times d}} \\
&\quad\le \|\sigma\big(\frac{dH_\varepsilon(\varphi(\cdot,t_n))}{d\varphi} - \frac{dH_\varepsilon(\varphi_h^n)}{d\varphi}\big)(I - \nabla\varphi\otimes\nabla\varphi)(\cdot,t_n)\|_{L^2(\Omega)^{d\times d}} \\
&\qquad + \|\sigma\frac{dH_\varepsilon(\varphi_h^n)}{d\varphi}(\nabla(\varphi(\cdot,t_n) - \varphi_h^n)\otimes\nabla\varphi(\cdot,t_n))\|_{L^2(\Omega)^{d\times d}} \\
&\qquad\quad + \|\sigma\frac{dH_\varepsilon(\varphi_h^n)}{d\varphi}(\nabla\varphi(\cdot,t_n)\otimes\nabla(\varphi(\cdot,t_n) - \varphi_h^n))\|_{L^2(\Omega)^{d\times d}} \\
&\qquad\qquad + \|\sigma\frac{dH_\varepsilon(\varphi_h^n)}{d\varphi}(\nabla(\varphi(\cdot,t_n) - \varphi_h^n)\otimes\nabla(\varphi(\cdot,t_n) - \varphi_h^n))\|_{L^2(\Omega)^{d\times d}}.
\end{aligned}$$

We observe that $\dfrac{dH_\varepsilon}{d\varphi}$ is also Lipschitz-continuous, with bounded Lipschitz constant (by $\frac{\pi}{2\varepsilon^2}$). We use Proposition 5.2 for the first term, Proposition 5.3 (with $p = 4$ for instance) for the last three terms, and obtain the desired result. □

To go further and in order to obtain the error estimate $\|\boldsymbol{u}(.,t_n) - \boldsymbol{u}_h^n\|$ at time t_n, we subtract the first line of (4.33) from the first line of equation (3.21), which gives for any $\boldsymbol{v}$ in $\mathbb{X}_h^n$,

$$\begin{aligned}
&\int_\Omega \Big(\rho(\varphi)(\boldsymbol{x},t_n)\big(\frac{\partial\boldsymbol{u}}{\partial t} + \boldsymbol{u}\cdot\nabla\boldsymbol{u}\big)(\boldsymbol{x},t_n) - \rho(\varphi_h^n)(\boldsymbol{x})\big(\frac{\boldsymbol{u}_h^n - \tilde{\boldsymbol{u}}_h^{n-1}}{\tau_n}\big)(\boldsymbol{x})\Big)\boldsymbol{v}(\boldsymbol{x})\,d\boldsymbol{x} \\
&\quad - \int_\Omega (\nabla\cdot\boldsymbol{v})(\boldsymbol{x})\big(p(\boldsymbol{x},t_n) - p_h^n(\boldsymbol{x})\big)\,d\boldsymbol{x} \\
&\qquad + \int_\Omega \Big(\nu(\varphi)(\boldsymbol{x},t_n)\nabla\boldsymbol{u}(\boldsymbol{x},t_n) - \nu(\varphi_h^n)(\boldsymbol{x})\nabla\boldsymbol{u}_h^n(\boldsymbol{x})\Big) : \nabla\boldsymbol{v}(\boldsymbol{x})\,d\boldsymbol{x} \\
&\qquad\quad = \int_\Omega \big(T(\varphi(\boldsymbol{x},t_n)) - T(\varphi_h^n)(\boldsymbol{x})\big) : \nabla\boldsymbol{v}(\boldsymbol{x})\,d\boldsymbol{x}.
\end{aligned} \tag{5.45}$$

The key idea consists in inserting in this equation the mean value

$$M_n(\boldsymbol{x}) = \frac{1}{\tau_n}\int_{t_{n-1}}^{t_n} \big(\frac{\partial\boldsymbol{u}}{\partial t} + \boldsymbol{u}\cdot\nabla\boldsymbol{u}\big)(\boldsymbol{x},t)\,dt.$$

Indeed, it is equal to

$$M_n(\boldsymbol{x}) = \frac{\boldsymbol{u}(\boldsymbol{x},t_n) - \boldsymbol{u}(X(\boldsymbol{x},t_n;t_{n-1}))}{\tau_n},$$

thus easier to compare to the discrete one, and standard arguments yield that, if $\boldsymbol{u}$ belongs to $H^2(t_{n-1},t_n;L^2(\Omega)^d)$ and C_n denotes its norm in this space then

$$\|(\frac{\partial \boldsymbol{u}}{\partial t}+\boldsymbol{u}\cdot\nabla\boldsymbol{u})(\cdot,t_n)-M_n\|_{L^2(\Omega)^d}\leq C_n\tau_n. \tag{5.46}$$

Proposition 5.5. *Assume that the solution φ of problem (3.17) satisfies (5.39) and that the solution $(\boldsymbol{u},p)$ of problem (3.20) – (3.21) is such that*

$$\begin{aligned}\boldsymbol{u}\in W^{1,\infty}(\,\Omega\times]0,T_f[\,)\cap H^2(0,T_f;L^2(\Omega)^d)\cap L^\infty(0,T_f;H^2(\Omega)^d),\\ p\in L^\infty(0,T_f;H^2(\Omega)).\end{aligned} \tag{5.47}$$

Then, the following estimate holds for $1\leq n\leq N$

$$\begin{aligned}&\Big(\tau_n^{-1}\|\boldsymbol{u}(\cdot,t_n)-\boldsymbol{u}_h^n\|^2_{L^2(\Omega)^d}+|\boldsymbol{u}(\cdot,t_n)-\boldsymbol{u}_h^n|^2_{H^1(\Omega)^d}\Big)^{\frac12}\\ &\quad\leq C\,(h_n+\tau_n+\frac{h_n^2}{\tau_n})+c\,(\frac{\varepsilon_1^n}{\varepsilon^2}+\frac{\varepsilon_2^n}{\varepsilon})+(\tau_n^{-1})^{\frac12}\|\boldsymbol{u}(\cdot,t_{n-1})-\boldsymbol{u}^{n-1}\|_{L^2(\Omega)^d},\end{aligned} \tag{5.48}$$

where the constant C only depends on the regularity of φ, $\boldsymbol{u}$ and p.

Proof. First, let us introduce the kernel space $\mathbb{V}_h^n$ of $b(\cdot,\cdot)$ in $\mathbb{X}_h^n$:

$$\mathbb{V}_h^n:=\left\{\boldsymbol{v}_h^n\in\mathbb{X}_h^n,\quad \forall q\in\mathbb{M}_h^n,\quad \int_\Omega(\nabla\cdot\boldsymbol{v}_h^n)(\boldsymbol{x})\,q(\boldsymbol{x})\,d\boldsymbol{x}=0\right\}.$$

Next, we add and subtract M_n in the first term of (5.45) and consider $\boldsymbol{v}=\boldsymbol{w}_h^n-\boldsymbol{u}_h^n$, for all $\boldsymbol{w}_h^n\in\mathbb{V}_h^n$, then we get

$$\begin{aligned}&\rho_1\tau_n^{-1}\|\boldsymbol{w}_h^n-\boldsymbol{u}_h^n\|^2_{L^2(\Omega)^d}+\nu_1|\boldsymbol{w}_h^n-\boldsymbol{u}_h^n|^2_{H^1(\Omega)^d}\\ &\quad=-\tau_n^{-1}\int_\Omega\rho(\varphi_h^n)(\boldsymbol{x})\big(\boldsymbol{u}(\boldsymbol{x},t_n)-\boldsymbol{w}_h^n(\boldsymbol{x})\big)\,(\boldsymbol{w}_h^n-\boldsymbol{u}_h^n)\,(\boldsymbol{x})\,d\boldsymbol{x}\\ &\quad-\int_\Omega\nu(\varphi_h^n)(\boldsymbol{x},t_n)\,(\nabla(\boldsymbol{u}(\boldsymbol{x},t_n)-\boldsymbol{w}_h^n(\boldsymbol{x}))):\nabla\,(\boldsymbol{w}_h^n-\boldsymbol{u}_h^n)\,(\boldsymbol{x})\,d\boldsymbol{x}\\ &\quad+\int_\Omega(T(\varphi)(\boldsymbol{x},t_n)-T(\varphi_h^n)(\boldsymbol{x})):\nabla\,(\boldsymbol{w}_h^n-\boldsymbol{u}_h^n)\,(\boldsymbol{x})\,d\boldsymbol{x}\\ &\quad-\int_\Omega\rho(\varphi)(\boldsymbol{x},t_n)\left((\frac{\partial\boldsymbol{u}}{\partial t}+\boldsymbol{u}\cdot\nabla\boldsymbol{u})(\boldsymbol{x},t_n)-M_n\right)\cdot(\boldsymbol{w}_h^n-\boldsymbol{u}_h^n)\,(\boldsymbol{x})\,d\boldsymbol{x}\\ &\quad+\int_\Omega(\nabla\cdot(\boldsymbol{w}_h^n-\boldsymbol{u}_h^n))\,(\boldsymbol{x})\;(p(\boldsymbol{x},t_n)-p_h^n(\boldsymbol{x}))\;d\boldsymbol{x}\\ &\quad-\int_\Omega(\nu(\varphi)(\boldsymbol{x},t_n)-\nu(\varphi_h^n)(\boldsymbol{x}))\;\nabla\boldsymbol{u}(\boldsymbol{x}):\nabla\,(\boldsymbol{w}_h^n-\boldsymbol{u}_h^n)\,(\boldsymbol{x})\,d\boldsymbol{x}\\ &\quad-\int_\Omega(\rho(\varphi)-\rho(\varphi_h^n))\;M_n\;(\boldsymbol{w}_h^n-\boldsymbol{u}_h^n)\,(\boldsymbol{x})\,d\boldsymbol{x}\\ &\quad+\int_\Omega\rho(\varphi_h^n)(\boldsymbol{x})\left(\frac{\boldsymbol{u}(X(\boldsymbol{x},t_n;t_{n-1}))-\tilde{\boldsymbol{u}}_h^{n-1}(\boldsymbol{x})}{\tau_n}\right)(\boldsymbol{w}_h^n-\boldsymbol{u}_h^n)\,(\boldsymbol{x})\,d\boldsymbol{x}\\ &\quad=\sum_{j=1}^8 I_j.\end{aligned} \tag{5.49}$$

Using successively Cauchy–Schwarz and Holder inequalities together with Young's inequality, we bound each term $I_j, 1\leq j\leq 8$ in the right hand side as follow: $\forall\alpha>0$

$$\begin{aligned}I_1&\leq\rho_2\tau_n^{-1}\|\boldsymbol{u}(\cdot,t_n)-\boldsymbol{w}_h^n\|_{L^2(\Omega)^d}\|\boldsymbol{w}_h^n-\boldsymbol{u}_h^n\|_{L^2(\Omega)^d}\\ &\leq\tau_n^{-1}\left(\frac{\rho_2^2}{2\alpha}\|\boldsymbol{u}(\cdot,t_n)-\boldsymbol{w}_h^n\|^2_{L^2(\Omega)^d}+\frac{\alpha}{2}\|\boldsymbol{w}_h^n-\boldsymbol{u}_h^n\|^2_{L^2(\Omega)^d}\right)\end{aligned}$$

and

$$I_2 \leq \nu_2 |\boldsymbol{u}(\cdot,t_n) - \boldsymbol{w}_h^n|_{H^1(\Omega)^d} |\boldsymbol{w}_h^n - \boldsymbol{u}_h^n|_{H^1(\Omega)^d}$$
$$\leq \frac{\nu_2^2}{2\alpha} |\boldsymbol{u}(\cdot,t_n) - \boldsymbol{w}_h^n|^2_{H^1(\Omega)^d} + \frac{\alpha}{2} |\boldsymbol{w}_h^n - \boldsymbol{u}_h^n|^2_{H^1(\Omega)^d}.$$

Using (5.44), we have

$$I_3 \leq \|T(\varphi(\cdot,t_n)) - T(\varphi_h^n)\|_{L^2(\Omega)^d} |\boldsymbol{w}_h^n - \boldsymbol{u}_h^n|_{H^1(\Omega)^d}$$
$$\leq \frac{1}{2\alpha} \|T(\varphi(\cdot,t_n)) - T(\varphi_h^n)\|^2_{L^2(\Omega)^d} + \frac{\alpha}{2} |\boldsymbol{w}_h^n - \boldsymbol{u}_h^n|^2_{H^1(\Omega)^d}$$
$$\leq \frac{c}{2\alpha} \left(\frac{\varepsilon_1^n}{\alpha^2} + \frac{\varepsilon_2^n}{\alpha} \right)^2 + \frac{\alpha}{2} |\boldsymbol{w}_h^n - \boldsymbol{u}_h^n|^2_{H^1(\Omega)^d}.$$

Thanks to (5.46), I_4 can be bounded as follow

$$I_4 \leq \rho_2 \left\| \left(\frac{\partial \boldsymbol{u}}{\partial t} + \boldsymbol{u} \cdot \nabla \boldsymbol{u} \right)(\cdot,t_n) - M_n \right\|_{L^2(\Omega)^d} \|\boldsymbol{w}_h^n - \boldsymbol{u}_h^n\|_{L^2(\Omega)^d}$$
$$\leq \rho_2 C_P \left\| \left(\frac{\partial \boldsymbol{u}}{\partial t} + \boldsymbol{u} \cdot \nabla \boldsymbol{u} \right)(\cdot,t_n) - M_n \right\|_{L^2(\Omega)^d} |\boldsymbol{w}_h^n - \boldsymbol{u}_h^n|_{H^1(\Omega)^d}$$
$$\leq \frac{\rho_2^2 C_P^2}{2\alpha} \left\| \left(\frac{\partial \boldsymbol{u}}{\partial t} + \boldsymbol{u} \cdot \nabla \boldsymbol{u} \right)(\cdot,t_n) - M_n \right\|^2_{L^2(\Omega)^d} + \frac{\alpha}{2} |\boldsymbol{w}_h^n - \boldsymbol{u}_h^n|^2_{H^1(\Omega)^d}$$
$$\leq \frac{\rho_2^2 C_P^2}{2\alpha} \tau_n^2 + \frac{\alpha}{2} |\boldsymbol{w}_h^n - \boldsymbol{u}_h^n|^2_{H^1(\Omega)^d}.$$

Observe that the term I_5 involving the pressure can be written as

$$I_5 := -\int_\Omega (\nabla \cdot (\boldsymbol{w}_h^n - \boldsymbol{u}_h^n))(\boldsymbol{x}) \big(p(\boldsymbol{x},t_n) - p_h^n(\boldsymbol{x}) \big)\, d\boldsymbol{x}$$
$$= -\int_\Omega (\nabla \cdot (\boldsymbol{w}_h^n - \boldsymbol{u}_h^n))(\boldsymbol{x}) \big(p(\boldsymbol{x},t_n) - \mathcal{I}_h^n p(\boldsymbol{x}) \big)\, d\boldsymbol{x}.$$

Then,

$$I_5 \leq \frac{1}{2\alpha} \|p(\cdot,t_n) - \mathcal{I}_h^n p(\cdot,t_n)\|^2 + \frac{\alpha}{2} |\boldsymbol{w}_h^n - \boldsymbol{u}_h^n|^2_{H^1(\Omega)^d}.$$

From (5.43), we deduce that

$$I_6 \leq \|\nu(\varphi)(\cdot,t_n) - \nu(\varphi_h^n)\|_{L^\infty(\Omega)} |\boldsymbol{u}|^2_{H^1(\Omega)^d} |\boldsymbol{w}_h^n - \boldsymbol{u}_h^n|_{H^1(\Omega)^d}$$
$$\leq \frac{1}{2\alpha} |\boldsymbol{u}|^2_{H^1(\Omega)^d} \|\nu(\varphi)(\cdot,t_n) - \nu(\varphi_h^n)\|^2_{L^\infty(\Omega)} + \frac{\alpha}{2} |\boldsymbol{w}_h^n - \boldsymbol{u}_h^n|^2_{H^1(\Omega)^d}$$
$$\leq \frac{1}{2\alpha} |\boldsymbol{u}|^2_{H^1(\Omega)^d} \frac{\varepsilon_1^{n\,2}}{\alpha} + \frac{\alpha}{2} |\boldsymbol{w}_h^n - \boldsymbol{u}_h^n|^2_{H^1(\Omega)^d}$$

and owing to (5.43), we get

$$I_7 \leq \|\rho(\varphi) - \rho(\varphi_h^n))\|_{L^\infty(\Omega)} \|M_n\|_{L^2(\Omega)^d} \|\boldsymbol{w}_h^n - \boldsymbol{u}_h^n\|_{L^2(\Omega)^d}$$
$$\leq \tau_n^{-1} c(\boldsymbol{u}) \|\rho(\varphi) - \rho(\varphi_h^n))\|_{L^\infty(\Omega)} \|\boldsymbol{w}_h^n - \boldsymbol{u}_h^n\|_{L^2(\Omega)^d}$$
$$\leq \tau_n^{-1} \left(\frac{c(\boldsymbol{u})^2}{2\alpha} \|\rho(\varphi) - \rho(\varphi_h^n))\|^2_{L^\infty(\Omega)} + \frac{\alpha}{2} \|\boldsymbol{w}_h^n - \boldsymbol{u}_h^n\|^2_{L^2(\Omega)^d} \right)$$
$$\leq \frac{c(\boldsymbol{u})^2}{2\alpha^2} \tau_n^{-1} \varepsilon_1^n + \frac{\alpha}{2} \tau_n^{-1} \|\boldsymbol{w}_h^n - \boldsymbol{u}_h^n\|^2_{L^2(\Omega)^d}.$$

Now, in order to estimate I_8, we will bound $\left\|\boldsymbol{u}(X(\cdot,t_n;t_{n-1}))-\tilde{\boldsymbol{u}}_h^{n-1}\right\|_{L^2(\Omega)^d}$. By triangle inequality, we have

$$\begin{aligned}\|\boldsymbol{u}(X(\cdot,t_n,t_{n-1}))-\tilde{\boldsymbol{u}}_h^{n-1}\|_{L^2(\Omega)^d} &\le \|\boldsymbol{u}(X(\cdot,t_n,t_{n-1}))-\boldsymbol{u}(X_h^n)\|_{L^2(\Omega)^d}\\ &\quad+\|\boldsymbol{u}(X_h^n)-\boldsymbol{u}_h^{n-1}(X_h^n)\|_{L^2(\Omega)^d}+\|\boldsymbol{u}_h^{n-1}(X_h^n))-\tilde{\boldsymbol{u}}_h^{n-1}\|_{L^2(\Omega)^d}.\end{aligned}$$

Using the mean value theorem for the first term, we obtain

$$\|\boldsymbol{u}(X(\cdot,t_n,t_{n-1}))-\boldsymbol{u}(X_h^n)\|_{L^2(\Omega)^d}\le\|\nabla\boldsymbol{u}\|_\infty\|X(\cdot,t_n,t_{n-1})-X_h^n\|_{L^2(\Omega)^d}$$

We write

$$\boldsymbol{x}-X(\boldsymbol{x},t_n;t_{n-1})=\int_{t_{n-1}}^{t_n}\boldsymbol{u}(X(\boldsymbol{x},t_n,t),t)dt\simeq\tau_n\boldsymbol{u}(X(\boldsymbol{x},t_n,t_n),t_n)=\tau_n\boldsymbol{u}(\boldsymbol{x},t).$$

On the other hand, we have from (4.27)

$$\boldsymbol{x}-X_h^n(\boldsymbol{x},t_n;t_{n-1})=\tau_n\boldsymbol{u}_h^{n-1}(\boldsymbol{x}).$$

Thus, we have from [6, Chap. IX, lemme 1.1]

$$\|\boldsymbol{u}_h^{n-1}(X_h^n)-\tilde{\boldsymbol{u}}_h^{n-1}\|_{L^2(\Omega)^d}\le ch_n\|\boldsymbol{u}_h^{n-1}\|_{H^1(\Omega)^d}.$$

We conclude by choosing an adequate nonnegative real number α and combining all obtained bounds of $(I_j)_{1\le j\le 8}$ with the triangle inequality and interpolation estimates. □

Remark 5.6. *Owing to the inf-sup condition (4.36), an error estimate for the pressure $p(\cdot,t_n)-p_h^n$ can also be derived, we skip it for brevity.*

We observe that the estimate (5.48) contains error terms at time t_{n-1}, so we need an induction on n to conclude. We denote by h the maximum of the h_n, $0\le n\le N$.

Theorem 5.7. *Assume that the solution $(\varphi,\boldsymbol{u},p)$ of problem (3.17)-(3.20)-(3.21) is such that*

$$\begin{aligned}&\varphi\in\mathcal{C}^0(0,T_f;W^{2,\infty}(\Omega)),\ p\in L^\infty(0,T_f;H^2(\Omega))\\ &\text{and}\qquad\boldsymbol{u}\in W^{1,\infty}(\Omega\times]0,T_f[)\cap H^2(0,T_f;L^2(\Omega)^d)\cap\mathcal{C}^0(0,T_f;H^2(\Omega)^d).\end{aligned}\tag{5.50}$$

$$p\in L^\infty(0,T_f;H^2(\Omega)).\tag{5.51}$$

For $1\le n\le N$, let us choose the parameters τ and h such that,

$$h\le c\,\hbar_n,\qquad|\tau|\le c\,\hbar_n^2.\tag{5.52}$$

Then, the following estimates hold for $1\le n\le N$

$$\|\varphi(\cdot,t_n)-\varphi_h^n\|_{L^\infty(\Omega)}\le C_n\,(h^2+|\tau|),\tag{5.53}$$

$$\|\boldsymbol{u}(\cdot,t_n)-\boldsymbol{u}_h^n\|_{H^1(\Omega)^d}\le C_n\,(h+|\tau|),\tag{5.54}$$

where the constant C_n depends on the regularity of φ, $\boldsymbol{u}$ and p, and also on n.

Proof. We proceed by induction on n.
1) For $n=0$, estimates (5.53) and (5.54) are obvious since φ_h^0 and $\boldsymbol{u}_h^0$ are the interpolates of φ_0 and $\boldsymbol{u}_0$, respectively.
2) Assume that (5.53) and (5.54) hold for $n-1$. We use the following inverse inequality (with $\eta>0$)

$$\begin{aligned}\|\boldsymbol{u}_h^{n-1}\|_{L^\infty(\Omega)^d}&\le\|\boldsymbol{w}_h\|_{L^\infty(\Omega)^d}\\ &\quad+\hbar_{n-1}^{1-(\frac{d}{2}+\eta)}\left(\|\boldsymbol{u}(\cdot,t_{n-1})-\boldsymbol{w}_h\|_{H^1(\Omega)^d}+\|\boldsymbol{u}(\cdot,t_{n-1})-\boldsymbol{u}_h^{n-1}\|_{H^1(\Omega)^d}\right),\end{aligned}\tag{5.55}$$

where $\boldsymbol{w}_h$ is any approximation of $\boldsymbol{u}(\cdot,t_{n-1})$ in $\mathbb{X}_h^{n-1}$. By triangle inequality and the Sobolev embedding from H^2 into L^∞, the first term in the above inequality is bounded as follow:

$$\begin{aligned}\|\boldsymbol{w}_h\|_{L^\infty(\Omega)^d} &\le c\|\boldsymbol{w}_h-\boldsymbol{u}(\cdot,t_{n-1})\|_{L^\infty(\Omega)^d}+c\|\boldsymbol{u}(\cdot,t_{n-1})\|_{L^\infty(\Omega)^d}\\ &\le c(h^{2-\frac{d}{2}}+1)\|\boldsymbol{u}(\cdot,t_{n-1})\|_{H^2(\Omega)^d}.\end{aligned}\tag{5.56}$$

To evaluate the second term, we derive from the approximation estimates that

$$\hbar_{n-1}^{1-(\frac{d}{2}+\eta)}\,\|\boldsymbol{u}(\cdot,t_{n-1})-\boldsymbol{w}_h\|_{H^1(\Omega)^d}\le c\hbar_{n-1}^{1-(\frac{d}{2}+\eta)}\,h_{n-1}\,\|\boldsymbol{u}(\cdot,t_{n-1})\|_{H^2(\Omega)^d}.\tag{5.57}$$

Owing to (5.52), we obtain

$$\hbar_{n-1}^{1-(\frac{d}{2}+\eta)}\,\|\boldsymbol{u}(\cdot,t_{n-1})-\boldsymbol{w}_h\|_{H^1(\Omega)^d}\le ch^{2-(\frac{d}{2}+\eta)}\,\|\boldsymbol{u}(\cdot,t_{n-1})\|_{H^2(\Omega)^d}.\tag{5.58}$$

We use the induction assumption and (5.52) to estimate the third term:

$$\begin{aligned}\hbar_{n-1}^{1-(\frac{d}{2}+\eta)}\,\left\|\boldsymbol{u}(\cdot,t_{n-1})-\boldsymbol{u}_h^{n-1}\right\|_{H^1(\Omega)^d}&\le C_{n-1}\,\hbar_{n-1}^{1-(\frac{d}{2}+\eta)}\,(h+|\tau|)\\ &\le C_{n-1}\,h^{1-(\frac{d}{2}+\eta)}\,(h+|\tau|)\,.\end{aligned}\tag{5.59}$$

From (5.55), (5.56), (5.58) and (5.59), we deduce that $\|\boldsymbol{u}_h^{n-1}\|_{L^\infty(\Omega)^d}$ is bounded and

$$\tau_n\|\boldsymbol{u}_h^{n-1}\|_{L^\infty(\Omega)^d}\le C_n\tau_n\quad\text{and}\quad\hbar_n^{-1}\,\tau_n\|\boldsymbol{u}_h^{n-1}\|_{L^\infty(\Omega)^d}\le C_n\hbar_n^{-1}\tau_n\le\hbar_n.$$

Next, inserting the induction hypothesis in (5.40) and (5.48) gives (5.53) and (5.54), respectively. □

Despite the technicity of the proofs, estimates (5.53) and (5.54) are fully optimal. But condition (5.52) is too restrictive: it involves both a hard Courant–Friedrichs–Lévy (CFL) condition and the uniform regularity of the family of triangulations. Fortunately the same arguments as in the previous proof lead to the following result.

Corollary 5.8. *Assume that the solution $(\varphi,\boldsymbol{u},p)$ of problem (3.17) – (3.20) – (3.21) satisfies (5.50). For $1\le n\le N$, let us choose the parameters τ and h such that, for a positive constant η,*

$$h^2+|\tau|\le c\,\hbar_n{}^{\frac{d}{2}+\eta}.\tag{5.60}$$

Then, the following estimates hold for $1\le n\le N$

$$\|\varphi(\cdot,t_n)-\varphi_h^n\|_{L^\infty(\Omega)}\le C_n\,(h^2+|\tau|),\tag{5.61}$$

$$\text{and}\qquad\|\boldsymbol{u}(\cdot,t_n)-\boldsymbol{u}_h^n\|_{H^1(\Omega)^d}\le C_n\,\hbar_n{}^{-1}(h^2+|\tau|),\tag{5.62}$$

where the constant C_n depends on the regularity of φ, $\boldsymbol{u}$ and p, and also on n.

Proof. By the same arguments used in the previous proof, we establish by induction on n (5.61) and (5.62). Combining (5.57) and (5.60), this yields

$$\hbar_{n-1}^{1-(\frac{d}{2}+\eta)}\,\|\boldsymbol{u}(\cdot,t_{n-1})-\boldsymbol{w}_h\|_{H^1(\Omega)^d}\le c\hbar_{n-1}\,h^{-2}\,h_{n-1}.\le c.$$

Owing to induction hypothesis and (5.60)

$$\begin{aligned}\hbar_{n-1}^{1-(\frac{d}{2}+\eta)}\,\left\|\boldsymbol{u}(\cdot,t_{n-1})-\boldsymbol{u}_h^{n-1}\right\|_{H^1(\Omega)^d}&\le C_{n-1}\,\hbar_{n-1}^{1-(\frac{d}{2}+\eta)}\,\hbar_{n-1}^{-1}\,\left((h^2+|\tau|\right)\\ &\le C_{n-1}.\end{aligned}$$

Then, $\|\boldsymbol{u}_h^{n-1}\|_{L^\infty(\Omega)^d}$ is bounded. This conclude the proof. □

Assumption (5.60) is much more realistic and the convergence of the discretization holds for standard properties of the family of triangulation.

Remark 5.9. *The fact that the constant C_n in estimates (5.53), (5.54), (5.61) and (5.62) depends on n can be avoided either by weakly strengthening conditions (5.52) and (5.60) or working with specific family of parameters: for instance, it can be assumed that the quantity $h_n^2+\tau_n$ decreases with n.*

6. Numerical results

We now concentrate on the numerical properties of the discretization suggested above. We present three numerical tests. The first simulation is based on a manufactured solution in order to compute the time and space accuracy order of the algorithm. In the second and third tests, the Rayleigh–Taylor problem (RTP), see for instance [43] and the rising bubble [25], illustrate the numerical relevance of the proposed algorithm as we produce results comparable to the literature for this well known tests.

All numerical simulations are done using the software Freefem++ [23].

6.1. Time and space accuracy

This subsection is devoted to adding a quantitative flavor to Theorem 5.7 and Corollary 5.8 by determining numerically the convergence rates obtained in (5.53), (5.54)(or (5.62)). However, in the absence of analytical solutions, which are very hard to come by for this model, we decide to build an reference solution which will be our exact solution.

We use the square domain $\Omega = (-1,1)^2$ and we consider the system (2.11) with:

$$(\nu_1,\nu_2) = (1,1),\ (\rho_1,\rho_2) = (1,3),\ \sigma = 0.1 \text{ and } \varepsilon = 0.1.$$

and suitable forcing functions such that the exact solution is given by

$$\begin{aligned}
\varphi &= 2 + \sin(t)\,\cos(\pi x)\,\cos(\pi\, y)\\
u_1 &= \pi \sin(t)\,\sin(2\pi y)\,\sin(\pi x)\,\sin(\pi x)\\
u_2 &= -\pi \sin(t)\,\sin(2\pi x)\,\sin(\pi y)\,sin(\pi y)\\
p &= \sin(t)\,\cos(\pi x)\,\sin(\pi y).
\end{aligned}$$

In order to link the spatial and temporal refinements together, we introduce the following quantities

$$\begin{aligned}
\mathcal{E}_\varphi(h,\tau) &= h^2 + \tau,\\
\mathcal{E}_u(h,\tau) &= h + \tau.
\end{aligned} \tag{6.63}$$

First, dividing successively the uniform time step τ by four and the mesh size h by two, the convergence order is then estimated by:

$$\mathcal{O}_{h,\tau}(\varphi) = \log\left(\frac{\mathcal{E}_\varphi(h,\tau)}{\mathcal{E}_\varphi(h/2,\tau/4)}\right) = 2.$$

Simillary, to obtain the convergence order of the velocity, the couple (τ, h) was halved successively:

$$\mathcal{O}_{h,\tau}(\boldsymbol{u}) = \log\left(\frac{\mathcal{E}_u(h,\tau)}{\mathcal{E}_u(h/2,\tau/2)}\right) = 1.$$

The results of the velocity error in H^1-norm and the position of the interface error in L^∞-norm are given respectively in Tables 1 and 2. As predicted by (5.61) and (5.62) in Corollary 5.8, the estimates orders are observed for $\boldsymbol{u}$ and φ.

We can conclude that the numerical results are in concordance with our theoretical analysis.

6.2. Rayleigh–Taylor Problem

The widely used test problem for numerical simulations for two-fluid flow is the Rayleigh–Taylor problem (RTP), see for instance [43]. When a layer of heavier fluid is placed on top of another lighter layer in a gravitational field with gravity pointing downward, the initial planar interface is unstable. Any disturbance will grow to produce spikes of heavier fluid moving downwards and bubbles of lighter fluid moving upwards.

Table 1: Accuracy test of the velocity

τ	h	$\|\boldsymbol{u}_h - \boldsymbol{u}\|_{H^1(\Omega)}$	$\mathcal{O}_{h,\tau}(\boldsymbol{u})$
0.01	0.1	0.307	...
$\tau/2$	$h/2$	0.088	1.80
$\tau/4$	$h/4$	0.0288	1.61
$\tau/8$	$h/8$	0.0116	1.3
$\tau/16$	$h/16$	0.0054	1.1
$\tau/20$	$h/20$	0.00428ß	1.04

Table 2: Accuracy test of φ

τ	h	$\|\varphi_h - \varphi\|_{L^\infty(\Omega)}$	$\mathcal{O}_{h,\tau}(\varphi)$
0.01	0.1	0.00038	...
$\tau/4$	$h/2$	4.95e-05	2.95
$\tau/16$	$h/4$	6.33e-06	2.97
$\tau/64$	$h/8$	1.22e-06	2.37
$\tau/256$	$h/16$	3.e-07	2.04

This is the so-called Rayleigh–Taylor instability. In this test case a heavy fluid is placed on the top of a light fluid and the initial position of the perturbed interface between two fluids is

$$\varphi(\boldsymbol{x}) = \tanh \frac{y - 2 - 0.1\cos(2\pi\, x)}{0.01\sqrt{2}}.$$

The computational domain is the rectangle $\Omega =]0,1[\times]0,4[$ and the density difference is normally represented by the Atwood number $At = \dfrac{\rho_2 - \rho_1}{\rho_2 + \rho_1}$, where $\rho_2 > \rho_1$ correspond to the heavier and lighter fluids, respectively. We also introduce the following Reynolds number $Re = \dfrac{\rho_1 a^{\frac{3}{2}} g^{\frac{1}{2}}}{\nu}$. According to [43], the governing equations are made dimensionless by using the following references: $\rho_{ref} = \rho_1$, $a_{ref} = a$ and $t_{ref} = t\sqrt{a\,At\,g}$. A no-slip condition $\boldsymbol{u} = (0,0)$ is enforced at the bottom and top walls while the first component of velocity $u_1 = 0$ is imposed on the two vertical sides, which correspond to $\boldsymbol{u}\cdot\boldsymbol{n} = 0$. The time step τ_n is taken uniform and equal to $\Delta t = 0.01$. Also, we consider an uniform triangulation of the domain which consists of 50×200 regular grid. Finally, we work with $\varepsilon = 0.05$ and $\sigma = 0$. The interface shape at different dimensional times (for instance, $t = 0s, 1s, 2s, 3s, 4s$) are plotted in Figure 2. In the first one, the Reynolds number Re is equal to 100 and the Atwood number is equal to $At = 0.3$, while in the second one we take $Re = 1000$ and $At = 0.5$. During the early stages, the growth of the interface is slow and remains symmetrical. However, the characteristic mushroom shape emerges in the vicinity of the central vortex. Later, the heavier fluid falls continuously and the lighter fluid keep rising to form bubbles along the vertical side boundary, and the heavier fluid begins to roll up into two counter–rotating vortices.

6.3. Two-dimensional rising bubble

The next application is a circular bubble rising in a viscous fluid. For this simulation, we use data from the numerical experiment of Hysing et al [25] where the bubble is initially circular with radius $r = 0.25$ and center coordinates $(0.5, 0.5)$ placed at the bottom of a rectangular domain $]0,1[\times]0,2[$ with another fluid of higher density and viscosity. Figure 3 illustrates the initial configuration of this problem and the boundary conditions we use.
The parameter ε is taken equal to 0.025. Buoyancy effects will make the drop move to the top of the domain and undergo some deformation. The result shape depends naturally on different physical parameters, for

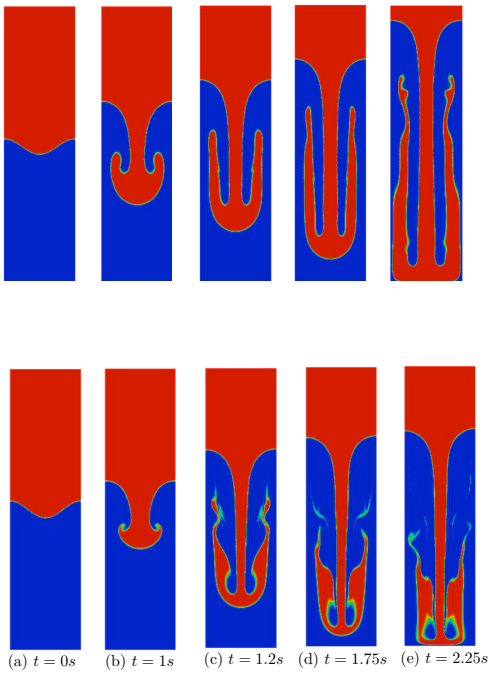

(a) $t = 0s$ (b) $t = 1s$ (c) $t = 1.2s$ (d) $t = 1.75s$ (e) $t = 2.25s$

Figure 2: Rayleigh-Taylor instability: Evolution of the interface shape in time. On the top: $At = 0.3$ and $Re = 100$. On the bottom $At = 0.5$ and $Re = 1000$

instance on Reynolds number $Re = \dfrac{2r\rho_1\sqrt{2rg}}{\nu_1}$ and on the so-called Eötvös number which gives the ratio of gravitational forces to surface tension effects $Eo = \dfrac{4r^2 g\rho_1}{\sigma}$. The density and viscosity of the heavy fluid are $\rho_1 = 1000, \nu_1 = 10$ whereas density and viscosity of the fluid occupied by the bubble are $\rho_2 = 1, \nu_2 = 0.1$. This yields $Re = 35$ and $Eo = 10$ (then the surface tension σ equal to 24.5).

Subsequently, we introduce the following quantities allowing the quantitative comparison with Hysing et al results [25]: the centroid or center of mass in order to track the translation of bubble

$$(x_c, y_c)(t) = \int_{\Omega_2} \boldsymbol{x} d\boldsymbol{x} \Big/ \int_{\Omega_2} d\boldsymbol{x}$$

and the rise velocity $u_2(x_c, y_c; t)$ which is the velocity component in the direction opposite to the gravitational vector.

The uniform time step $\tau_n = \Delta t = 0.0025$ and the initial triangulation of the domain consist of 100×200 regular grid of triangles adapted (local refinement, edge swapping and vertex suppression) based on the P2 interpolation of the initial value of

$$\varphi_0 = \tanh\left(\frac{\sqrt{(x-0.5)^2 + (y-0.5)^2} - 0.25}{2\varepsilon}\right).$$

Afterward, at each 5 times step, the mesh is adapted with respect to $(\boldsymbol{u}, \varphi)$ by metric control which is a standard function offered by FreeFEM++ [23]. The mesh generator uses Delaunay–type algorithms developed in [16, 17]. As expected the mesh is denser at the vicinity of the moving interface (see Figures 3 and 5).

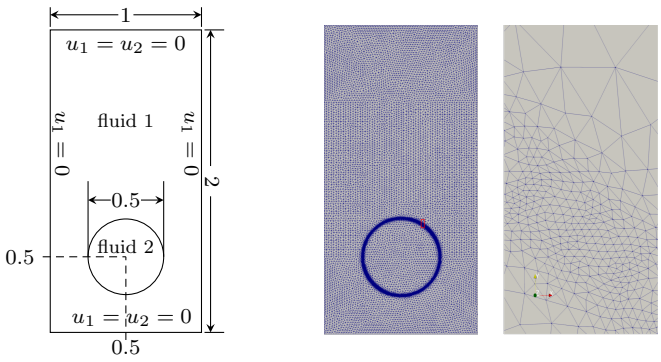

Figure 3: Rising bubble: geometry and illustration of an initial mesh obtained from the mesh adaptation based on the quadratic approximation of the analytical expression of φ_0. On the right a zoom of the interface region (red zone in the middle).

Furthermore, as usual, since the level set function φ may lose its hyperbolic tangent shape, we reinitialize it at each 5 times step by iterate few times (4 iterations) the time discrete formulation of equation (1.2) using an fictitious time step $\Delta t = 1e-4$.

The evolution of the bubble at different time t between $t = 0.6$ and $t = 3$ is presented in figure 4 and the corresponding adaptive mesh, see Figure 5. The evolution of the center of mass and rise velocity are presented in Figure 6. These results are similar to those obtain in [25].

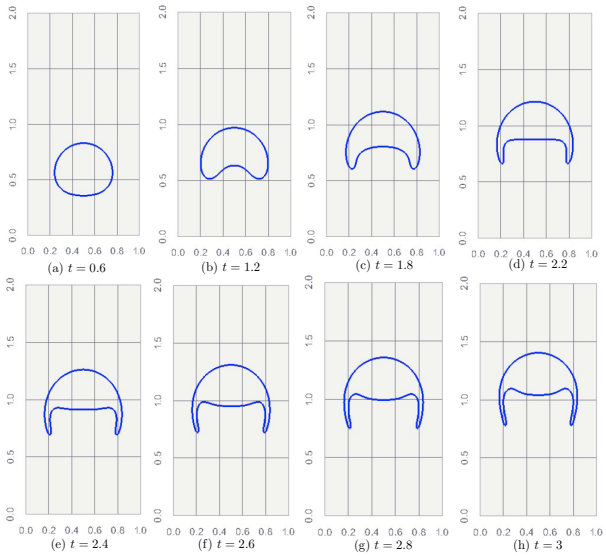

Figure 4: Evolution of the interface at different time

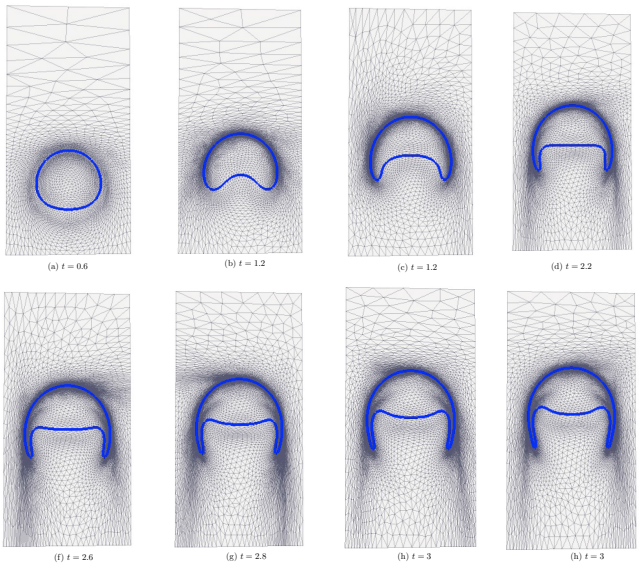

Figure 5: Typical time evolution of the adaptive mesh

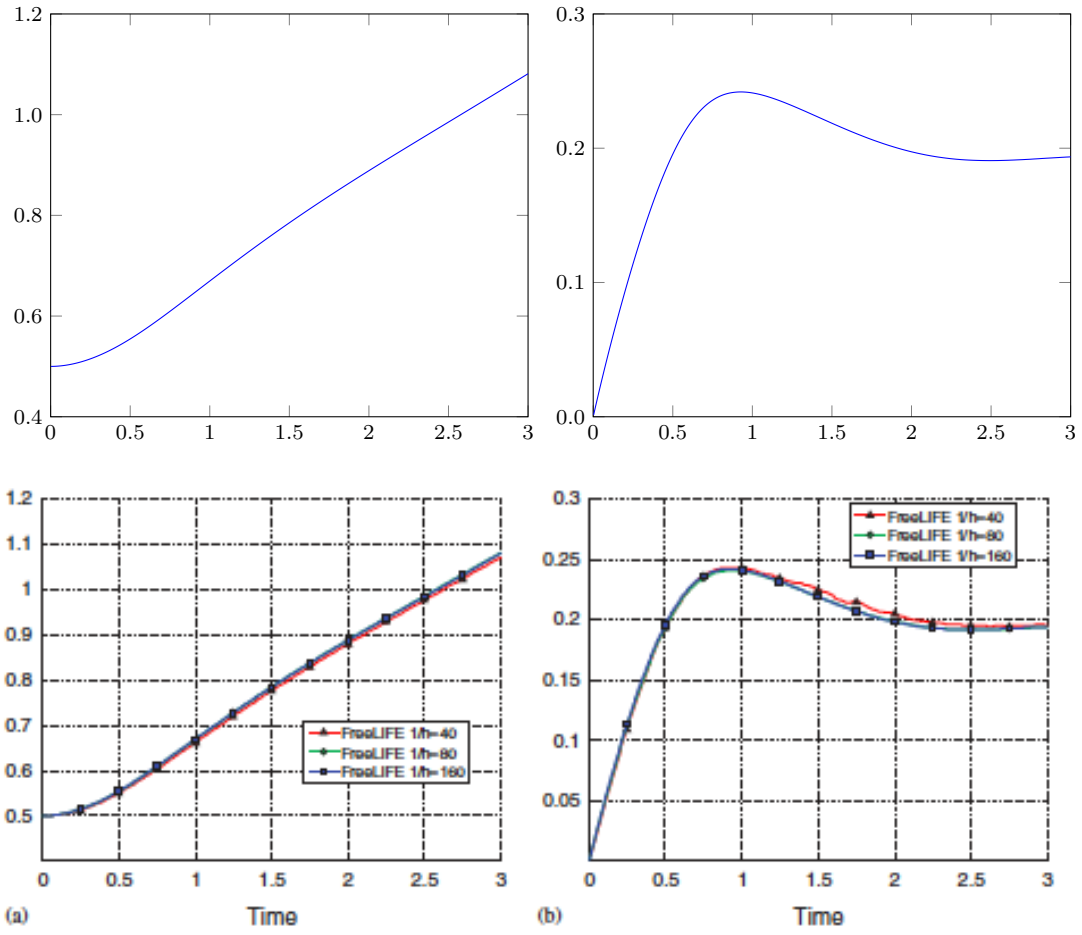

Figure 6: Rising bubble: evolution of : center of mass (left), rise velocity (right).
Present work on the top and Hysing et al [25] results on the bottom.

7. Conclusion

In this work, the analysis of the complex differential problem which governs the flow of two immiscible fluids including surface tension effects is presented. The nature of free–surface problem is faced adopting the level set method and the surface tension contribution in the momentum equation is accounted for using the CSF approach.

The well posedness of its variational formulation is proved under the rather restrictive condition of homogeneous Dirichlet boundary conditions.

The problem is discretized using the finite element method and the characteristics method is adopted to treat the advection terms in both the momentum and level set equations. We have performed its a priori error analysis and tested the convergence order using a manufactured solution approach. Finally, using the Rayleigh–Taylor problem and the single rising bubble as a benchmarks, we illustrated the relevance of the proposed method.

Acknowledgments

This paper is the fruit of our collaboration (S. Maarouf and D. Yakoubi) with our dear co–worker Christine Bernardi, who passed away while this paper was being expanded and revised version of Bernardi et al [5]. The authors S. Maarouf and D. Yakoubi thank Professor C. Bernardi for stimulating and fruitful discussions.

References

[1] R.A. Adams and J. F. Fournier. *Sobolev spaces*, volume 140 of *Pure and Applied Mathematics (Amsterdam)*. Elsevier/Academic Press, Amsterdam, second edition, 2003.

[2] H. Amann. *Ordinary differential equations*, volume 13 of *De Gruyter Studies in Mathematics*. Walter de Gruyter & Co., Berlin, 1990. An introduction to nonlinear analysis, Translated from the German by Gerhard Metzen.

[3] E. Bänsch. Finite element discretization of the Navier-Stokes equations with a free capillary surface. *Numer. Math.*, 88(2):203–235, 2001.

[4] J.W. Barrett, H. Garcke, and R. Nürnberg. A stable parametric finite element discretization of two-phase Navier-Stokes flow. *J. Sci. Comput.*, 63(1):78–117, 2015.

[5] C. Bernardi, S. Maarouf, and D Yakoubi. Finite element discretization of two immiscible fluids with surface tension. *HAL*, http://hal.upmc.fr/hal-01128264/document:1–36, 2015.

[6] C. Bernardi, Y. Maday, and F. Rapetti. *Discrétisations variationnelles de problèmes aux limites elliptiques*. Mathématiques et applications. Springer, Berlin, Heidelberg, 2004.

[7] K. Boukir, Y. Maday, B. Métivet, and E. Razafindrakoto. A high-order characteristics/finite element method for the incompressible Navier-Stokes equations. *Internat. J. Numer. Methods Fluids*, 25(12):1421–1454, 1997.

[8] F. Boyer and P. Fabrie. *Mathematical tools for the study of the incompressible Navier-Stokes equations and related models*, volume 183 of *Applied Mathematical Sciences*. Springer, New York, 2013.

[9] J. U. Brackbill, D. B. Kothe, and C. Zemach. A continuum method for modeling surface tension. *J. Comput. Phys.*, 100(2):335–354, 1992.

[10] G-H. Cottet, E. Maitre, and T. Milcent. Eulerian formulation and level set models for incompressible fluid-structure interaction. *M2AN Math. Model. Numer. Anal.*, 42(3):471–492, 2008.

[11] D. A. Di Pietro, S. Lo Forte, and N. Parolini. Mass preserving finite element implementations of the level set method. *Appl. Numer. Math.*, 56(9):1179–1195, 2006.

[12] R. J. DiPerna and P.L. Lions. Ordinary differential equations, transport theory and Sobolev spaces. *Invent. Math.*, 98(3):511–547, 1989.

[13] V. Doyeux, Y. Guyot, V. Chabannes, C. Prud'homme, and M. Ismail. Simulation of two-fluid flows using a finite element/level set method. Application to bubbles and vesicle dynamics. *J. Comput. Appl. Math.*, 246:251–259, 2013.

[14] J Eggers. Nonlinear dynamics and breakup of free–surface flows. *Rev. Mod. Phys*, 69:965–929, 1997.

[15] X. Feng. Fully discrete finite element approximations of the Navier-Stokes-Cahn-Hilliard diffuse interface model for two-phase fluid flows. *SIAM J. Numer. Anal.*, 44(3):1049–1072, 2006.

[16] P-J. Frey and P-L. George. *Maillage*. Editions Hermès, Paris, 1999.

[17] P-L. George and H. Borouchaki. *Delaunay triangulation and meshing*. Editions Hermès, Paris, 1998. Application to finite elements, Translated from the 1997 French original by the authors, P. J. Frey and Scott A. Canann.

[18] V. Girault and P.-A. Raviart. *Finite Element Methods for the Navier-Stokes Equations*, volume 5 of *Springer Series in Computational Mathematics*. Springer-Verlag, Berlin, 1986. Theory and algorithms.

[19] S. Gross, M.A. Olshanskii, and A. Reusken. A trace finite element method for a class of coupled bulk-interface transport problems. *ESAIM Math. Model. Numer. Anal.*, 49(5):1303–1330, 2015.

[20] S. Großand A. Reusken. An extended pressure finite element space for two-phase incompressible flows with surface tension. *J. Comput. Phys.*, 224(1):40–58, 2007.
[21] S. Gross and A. Reusken. Finite element discretization error analysis of a surface tension force in two-phase incompressible flows. *SIAM J. Numer. Anal.*, 45(4):1679–1700, 2007.
[22] M. Haddad, F. Hecht, and T. Sayah. Interface transport scheme of a two-phase flow by the method of characteristics. *Internat. J. Numer. Methods Fluids*, 83(6):513–543, 2017.
[23] F. Hecht. New development in freefem++. *Jour. Num. Math*, 20:251–266, 2012.
[24] T. Y. Hou, J. S. Lowengrub, and M. J. Shelley. Boundary integral methods for multicomponent fluids and multiphase materials. *J. Comput. Phys.*, 169(2):302–362, 2001.
[25] S. Hysing, S. Turek, D. Kuzmin, N. Parolini, E. Burman, S. Ganesan, and L. Tobiska. Quantitative benchmark computations of two-dimensional bubble dynamics. *Internat. J. Numer. Methods Fluids*, 60(11):1259–1288, 2009.
[26] M. Kirchhart, S. Gross, and A. Reusken. Analysis of an XFEM discretization for Stokes interface problems. *SIAM J. Sci. Comput.*, 38(2):A1019–A1043, 2016.
[27] B. Lafaurie, C. Nardone, R. Scardovelli, S. Zaleski, and G. Zanetti. Modelling merging and fragmentation in multiphase flows with SURFER. *J. Comput. Phys.*, 113(1):134–147, 1994.
[28] M Meier, G Yadigaroglu, and B.L Smith. A novel technique for including surface tension in plic-vof methods. *Eur. Jour. Mech - B/Fluids*, 21:61–73, 2002.
[29] T. Milcent. *Une approche eulérienne du couplage fluide-structure, analyse mathématique et applications en biomécanique*. PhD thesis, Université Joseph Fourier. Grenoble, 2009.
[30] S. Osher and R. Fedkiw. *Level set methods and dynamic implicit surfaces*, volume 153 of *Applied Mathematical Sciences*. Springer-Verlag, New York, 2003.
[31] S. Osher and J.A. Sethian. Fronts propagating with curvature-dependent speed: algorithms based on Hamilton-Jacobi formulations. *J. Comput. Phys.*, 79(1):12–49, 1988.
[32] O. Pironneau. On the transport-diffusion algorithm and its applications to the Navier-Stokes equations. *Numer. Math.*, 38(3):309–332, 1981/82.
[33] O. Pironneau and M. Tabata. Stability and convergence of a Galerkin-characteristics finite element scheme of lumped mass type. *Internat. J. Numer. Methods Fluids*, 64(10-12):1240–1253, 2010.
[34] S. Popinet and S. Zaleski. A front-tracking algorithm for accurate representation of surface tension. *Internat. J. Numer. Methods Fluids*, 30(6):775–793, 1999.
[35] A. Reusken. A finite element level set redistancing method based on gradient recovery. *SIAM J. Numer. Anal.*, 51(5):2723–2745, 2013.
[36] H. Rui and M. Tabata. A second order characteristic finite element scheme for convection-diffusion problems. *Numer. Math.*, 92(1):161–177, 2002.
[37] R. Scardovelli and S. Zaleski. Direct numerical simulation of free-surface and interfacial flow. In *Annual review of fluid mechanics, Vol. 31*, volume 31 of *Annu. Rev. Fluid Mech.*, pages 567–603. Annual Reviews, Palo Alto, CA, 1999.
[38] M. Schatzman. *Analyse numérique*. InterEditions, Paris, 1991. Cours et exercices pour la licence. [Course and exercises for the bachelor's degree].
[39] J. A. Sethian. *Level set methods and fast marching methods*, volume 3 of *Cambridge Monographs on Applied and Computational Mathematics*. Cambridge University Press, Cambridge, second edition, 1999. Evolving interfaces in computational geometry, fluid mechanics, computer vision, and materials science.
[40] M. Sussman. *A level set approach for computing solutions to incompressible two-phase flow*. ProQuest LLC, Ann Arbor, MI, 1994. Thesis (Ph.D.)–University of California, Los Angeles.
[41] C. Taylor and P. Hood. A numerical solution of the Navier-Stokes equations using the finite element technique. *Internat. J. Comput. & Fluids*, 1(1):73–100, 1973.
[42] R. Temam. *Navier-Stokes equations. Theory and numerical analysis*. North-Holland Publishing Co., Amsterdam-New York-Oxford, 1977. Studies in Mathematics and its Applications, Vol. 2.
[43] G. Tryggvason. Numerical simulation of the rayleigh–taylor instability. *J. Comput. Physics*, 75(2):253–282, 1988.
[44] G. Tryggvason, B. Bunner, A. Esmaeeli, D. Juric, N. Al-Rawahi, W. Tauber, J. Han, S. Nas, and Y.-J. Jan. A front-tracking method for the computations of multiphase flow. *J. Comput. Phys.*, 169(2):708–759, 2001.